J Comput Aided Mol Des (2013) 27:491–509
DOI 10.1007/s10822-013-9658-2

Approaching the 5-HT_3 receptor heterogeneity by computational studies of the transmembrane and intracellular domains

Marta Del Cadia · Francesca De Rienzo · Maria Cristina Menziani

Received: 11 December 2012 / Accepted: 11 June 2013 / Published online: 16 June 2013

Abstract 5-hydroxytryptamine type-3 receptor (5-HT_3), an important target of many neuroactive drugs, is a cation selective transmembrane pentamer whose functional stoichiometries and subunit arrangements are still debated, due to the extreme complexity of the system. The three dimensional structure of the 5-HT_3R subunits has not been solved so far. Moreover, most of the available structural and functional data is related to the extracellular ligand-binding domain, whereas the transmembrane and the intracellular receptor domains are far less characterised, although they are crucial for receptor function. Here, for the first time, 3D homology models of the transmembrane and the intracellular receptor domains of all the known human 5-HT_3 subunits have been built and assembled into homopentameric (5-HT_{3A}R, 5-HT_{3B}R, 5-HT_{3C}R, 5-HT_{3D}R and 5-HT_{3E}R) and heteropentameric receptors (5-HT_{3AB}, 5-HT_{3AC}, 5-HT_{3AD} and 5-HT_{3AE}), on the basis of the known three-dimensional structures of the nicotinic-acetylcholine receptor and of the ligand gated channel from *Erwinia chrysanthemi*. The comparative analyses of sequences, modelled structures, and computed electrostatic properties of the single subunits and of the assembled pentamers shed new light both on the stoichiometric composition and on the physicochemical requirements of the functional receptors. In particular, it emerges that a favourable environment for the crossing of the pore at the transmembrane and intracellular C terminus domain levels by Ca^{2+} ions is granted by the maximum presence of two B subunits in the 5-HT_3 pentamer.

Keywords Homology modelling · 5-HT_3 receptors · Electrostatic potential map · Energy profile

Introduction

The 5-hydroxytryptamine type-3 receptor (5-HT_3R) is a cation selective transmembrane protein which belongs to the Cys-loop LGIC (Ligand-Gated Ion Channel) family [1]. The nicotinic acetylcholine (nAChR), glycine (GlyR) and γ-aminobutyric type A ($GABA_A$R) receptors are the other members of the LGIC family, and they all share homologous amino acid sequences [2]. The LGICs play key roles in the physiology of a wide range of cells, especially those with excitable membranes, in fact they are responsible for fast synaptic transmission at chemical synapses and are important neuroactive drug targets [3].

The nAChR is the most studied LGIC and the best characterised, through pharmacological and molecular biological approaches. Moreover, the 4 Å resolution electron microscopy structure of a nAChR from *Torpedo marmorata* is available [4], therefore this receptor structure is often used as a prototype for the LGIC family. Recently, the structures of two prokaryotic LGICs and an eukaryotic LGIC have been determined by X-ray crystallography, providing other important model systems for the studies of the Cys-loop family: the pentameric structure of the ligand gated channel from *Erwinia chrysanthemi* (ELIC) [5], the pentameric structure from *Gloeobacter violaceus* (GLIC) [6] and the homopentameric glutamate-gated chloride channel α from *Caenorhabditis elegans* (GluCl) [7].

Electronic supplementary material The online version of this article (doi:10.1007/s10822-013-9658-2) contains supplementary material, which is available to authorized users.

M. Del Cadia · F. De Rienzo · M. C. Menziani (✉)
Dipartimento di Scienze Chimiche e Geologiche,
Università degli Studi di Modena e Reggio Emilia,
Via Campi 183, 41100 Modena, Italy
e-mail: menziani@unimore.it

In common with all members of the Cys-loop family, 5-HT_3Rs are assembled as a pseudo-symmetric pentamer formed by five subunits surrounding a central ion channel, which is permeable to small ions (Ca^{2+}, Na^{+}, K^{+}) [8, 9]. Each subunit is characterized by (1) a large extracellular N-terminal (extracellular, EC) domain, where the serotonin binding site is located, (2) a transmembrane (TM) domain, formed by four helices (TM1, TM2, TM3 and TM4) connected by the extracellular loop (TM2-TM3) and two intracellular linkers TM1-TM2 and TM3-TM4), and (3) an intracellular C terminus (IC) domain, which is formed by the long TM3-TM4 linker consisting of a large loop segment and a α-helical segment, called the MA-helix [3, 4, 10–13]. In each subunit, the pore-lining domain consists of the TM2 transmembrane α-helix, while the TM1, TM3 and TM4 helices keep it apart from the membrane [4, 14]. Amino acids within the α-helical portion of the IC domain (MA-helix) and within TM2 contribute to the ion permeation pathway [3].

In addition, the 5-HT_3Rs, similar to other LGICs, are gated, i.e. they switch between an activated (functional) open conformation, when the ligand binds to the receptor and the ions flow through the channel, and a non-activated closed conformation, in the absence of ligand binding, which precludes the ion flux [15]. When the ligand is continuously present in high concentrations, LGICs can also go into a desensitised and non-conducting state: the ligand is still bound, but the receptor is unable to conduct [15]. The channel opening-closing mechanism is still far from being completely understood. Very recently the structural mechanism of Ach-receptor gating has been determined by electron microscopy of ACh-sprayed and freeze-trapped postsynaptic membranes [16]. Although the low structure resolution (6.20 Å), the authors demonstrated that asymmetric helix movements triggered by Ach binding perturb the pore most at the level of the gate and in the nearby extracellular region, lowering the barrier for ion permeation. Only minimal adjustments to the pore are needed to obtain the measured conductance of the open-channel form; in fact it has been estimated an increasing of the diameter of the pore near the middle of the membrane, were the gate is located, by about 1 Å. This is in contrast with the results of previous experimental and theoretical studies which envisaged a twist of the TM2 helix triggered by ligand binding in the EC domain [17–20]. The nAChR gate is formed by rings of hydrophobic residues located at the centre of the TM2 helix [14], and several experiments proved that residues which are highly conserved across all LGICs have a critical role in channel function [12, 21, 22].

Five different 5-HT_3 receptor subunits, 5-HT_3A to E, have been identified so far, of which the most characterised is the A subunit, followed by the B subunit, while the first experiments involving the remaining three subunits have been carried out only recently [23, 24]. The subunit 5-HT_3A is capable of forming functional homopentameric receptors, while all the other 5-HT_3 subunits are functional only when coexpressed with the 5-HT_3A subunit [23–25]. The subunit stoichiometry of the heteropentameric 5-HT_3AB receptors has been identified to be: 2A:3B, with a BBABA arrangement [26]. However, this subunit arrangement has been brought into question by recent experimental site-directed mutagenesis studies [27, 28]; according to these, at least one AA interface for any 5-HT_3R is required to have a functional receptor.

Notwithstanding the large amount of information available, the 3D structure of the 5-HT_3R has not been solved yet, and most of the structural and functional data have been provided indirectly by studies on the nAChR, the prototypical Cys-loop receptor, although some computational and experimental studies have been also carried out directly on the 5-HT_3R. In particular, extensive computational [29–38] and experimental studies [8, 39–42] performed on the 5-HT_3R extracellular domain led to quite a vast and deep knowledge of this portion of the receptor. On the contrary, the TM and the IC receptor domains are far less characterised from both the experimental and computational points of view.

The aim of this work is to expand the knowledge about the 5-HT_3 family receptor, focusing on the structural features of the TM and IC domains, and hereafter to get new insights into the possible stoichiometric composition of the functional receptors and into the structural and electrostatic requirements for the channel to be entered by ions. The first step toward this aim is the construction of 3D homology models of the TM and IC regions for the human subunits 5-HT_3A to 5-HT_3E and the successive assembling of these modelled structures into homopentameric (5-HT_3A, 5-HT_3B, 5-HT_3C, 5-HT_3D and 5-HT_3E) and heteropentameric (5-HT_3AB, 5-HT_3AC, 5-HT_3AD and 5-HT_3AE) receptors. To our knowledge, no 3D structural model of the 5-HT_3 B, C, D and E subunit TM and IC domains has been built and reported in the literature, so far. Successively, the molecular electrostatic potential and the energetic profile of a cation along the pore channel of the homopentameric and heteropentameric receptors will be computed to attempt an interpretation of the process of the cation flux through the channel.

As a whole, the detailed comparison of the receptor subunit sequences and structures, together with the analysis of their physicochemical properties (i.e. molecular electrostatic potentials, energetic profile of the ion through the pore) will help us to interpret previous experimental data, to suggest possible explanations about the different behaviour shown by different receptors within the 5-HT_3 receptor family, and to make hypotheses

about the correlations of the receptor stoichiometry and functionality.

Methods and materials

Models building and refinements

The amino acid sequences of the TM and IC domains of the human 5-HT_3 receptor subunit A (UniProtKB entry: P46098), subunit B (UniProtKB entry: O95264), subunit C (UniProtKB entry: Q8WXA8), subunit D (UniProtKB entry: Q70Z44) and subunit E (UniProtKB entry: A5X5Y0) were extracted from the UniProtKB/Swiss-Prot [43] protein sequence database. These sequences were used to build structural homology models of the TM and IC portions of the human homomeric and heteromeric 5-HT_3 receptors. The available structures of the nAChR from *Torpedo Marmorata* (PDB entry: 2BG9) [4] and the ELIC (PDB entry: 2VL0) [5] were used as templates.

The sequence identity between ELIC and the 5-HT_3A subunit is lower (16 %) than that between nAChR and the 5-HT_3A subunit (i.e. 27 and 22 % for nAChR subunit β and ε, respectively), however both the structures were used because of the higher ELIC resolution with respect to that of nAChR (3.3 vs. 4.0 Å). The GLIC and GluCl structures, which have a sequence identity (to 5-HT_3A) similar to that of ELIC (16–18 %) but higher resolutions (2.90 and 3.26 Å), have not been taken into account because, in contrast to the other two structures, they show an open-pore folding [6, 7, 44].

A multiple alignment of 5-HT_3R subunit sequences, together with the sequences of the five chains of the nAChR structure and the ELIC subunit, was generated with ClustalW [45], using default parameters.

An insertion of amino acids of variable length depending on the 5-HT_3R subunit is present in the region between TM3 and TM4. Since in the nAChR structure the same region is only partially solved by electron microscopy (with the exception of the MA-helix, the atomic coordinates of most of this region are not available [4]), part of this stretch of amino acids has been deleted from the sequences. However, this deletion might compromise the correct modelling of the MA-helix. In view of these considerations, a structure-based alignment was also performed using the software MODELLER v. 9.10 [46], and putative helices were predicted, independently, by means TMHMM2 [47] and PSIPRED [48, 49]. Manual adjustments were then necessary to align both the sequence and structure of the MA-helices on the basis of the agreement between the results of the secondary structure prediction for 5-HT_3R (see Fig. 1) and the TM1-TM4 and MA-helix spatial positions of nAChR, and ELIC.

The residues finally included for each subunit are the following: A from 240 to 337 and from 418 to 478; B from 237 to 334 and from 381 to 441; C from 245 to 340 and from 405 to 447; D from 227 to 338 and from 403 to 454; E from 245 to 340 and from 405 to 456 (Fig. 1).

Modelling of the 5-HT_3A subunit was performed with the software MODELLER v 9.10 [46] using all the five chains of the nAChR structure and one chain of the ELIC structure (the five ELIC subunit are all identical) as templates. Twenty 3D models were generated for the 5-HT_3A subunit. The atomic coordinates of each model were optimized within the MODELLER program by making use of the conjugate gradients routine, and then refined using the "molecular dynamics with simulated annealing" routine [46].

All the 3D models obtained were checked against the available structural experimental information, such as the location of a few residues known to be involved in important functional roles by mutagenesis experiments. The position of these key residues was checked for all the modelled 5-HT_3A subunit structures in order to reject those structures which did not agree with the experimental information.

Subsequently, the 3D structures selected were also evaluated with the global G-factors and the Ramachandran plot residue distribution from the software PROCHECK [50], the objective function from MODELLER [46], the error values from ERRAT [51], and the global quality indicators from WHAT_CHECK [52, 53]. These technical indices are listed in the Online Resource. The 3D structures with the best agreement with experimental data[8] and the best technical evaluation score were selected and used for further analyses.

The 5-HT_3A model selected was used as template for modelling the human 5-HT_3B, 5-HT_3C, 5-HT_3D and 5-HT_3E TM and IC domains. Ten model structures were generated for each of these subunits, whose quality was assessed with the same technical checks used to select the 5-HT_3A model (see Online Resource). In addition, since nearly no experimental info is available for these subunit structures, the structural checks were performed by taking into account the residues corresponding (in the multiple sequence alignment) to the 5-HT_3A residues known to be relevant for function and/or structure.

Once selected the best 3D model structure for each subunit, the homopentamer (5-HT_3A, 5-HT_3B, 5-HT_3C, 5-HT_3D and 5-HT_3E) and the heteropentamer (5-HT_3AB, 5-HT_3AC, 5-HT_3AD and 5-HT_3AE) receptors were built by making use of the known structural constraints of nAChR (PDB: 2BG9). The AFM results obtained by Barrera et al. [26] for the 5-HT_3AB heteropentamer (2A:3B stoichiometry with a BBABA arrangement) were considered for the construction of the heteromeric receptors.

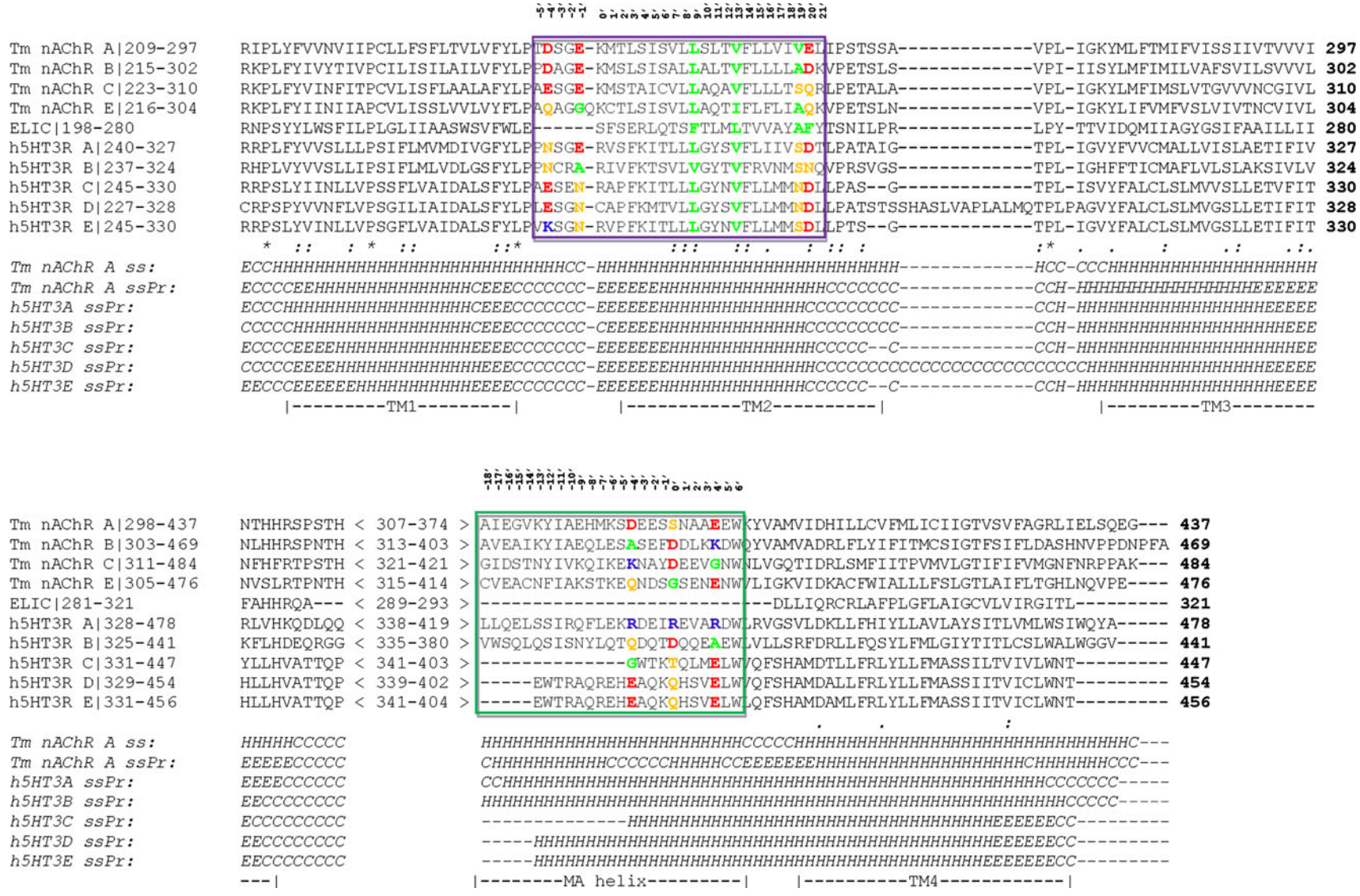
Tm nAChR A|209-297 RIPLYFVVNVIIPCLLFSFLTVLVFYLPTDSGE-KMTLSISVLLSLTVFLLVIVELIPSTSSA----------VPL-IGKYMLFTMIFVISSIIVTVVVI 297
Tm nAChR B|215-302 RKPLFYIVYTIVPCILISILAILVFYLPPDAGE-KMSLSISALLALTVFLLLLADKVPETSLS----------VPI-IISYLMFIMILVAFSVILSVVVL 302
Tm nAChR C|223-310 RKPLFYVINFITPCVLISFLAALAFYLPAESGE-KMSTAICVLLAQAVFLLLTSQRLPETALA----------VPL-IGKYLMFIMSLVTGVVVNCGIVL 310
Tm nAChR E|216-304 RKPLFYIINIIAPCVLISSLVVLVYFLPAQAGGQKCTLSISVLLAQTIFLFLIAQKVPETSLN----------VPL-IGKYLIFVMFVSLVIVTNCVIVL 304
ELIC|198-280 RNPSYYLWSFILPLGLIIAASWSVFWLE------SFSERLQTSFTLMLTVVAYAFYTSNILPR----------LPY-TTVIDQMIIAGYGSIFAAILLII 280
h5HT3R A|240-327 RRPLFYVVSLLLPSIFLMVMDIVGFYLPPNSGE-RVSFKITLLLGYSVFLIIVSDTLPATAIG----------TPL-IGVYFVVCMALLVISLAETIFIV 327
h5HT3R B|237-324 RHPLVYVVSLLIPSIFLMLVDLGSFYLPPNCRA-RIVFKTSVLVGYTVFRVNMSNQVPRSVGS----------TPL-IGHFFTICMAFLVLSLAKSIVLV 324
h5HT3R C|245-330 RRPSLYIINLLVPSSFLVAIDALSFYLPAESEN-RAPFKITLLLGYNVFLLMMNDLLPAS--G----------TPL-ISVYFALCLSLMVVSLLETVFIT 330
h5HT3R D|227-328 CRPSPYVVNFLVPSGILIAIDALSFYLPLESGN-CAPFKMTVLLGYSVFLLMMNDLLPATSTSSHASLVAPLALMQTPLPAGVYFALCLSLMVGSLLETIFIT 328
h5HT3R E|245-330 RRPSLYVINLLVPSGFLVAIDALSFYLPVKSGN-RVPFKITLLLGYNVFLLMMSDLLPTS--G----------TPL-IGVYFALCLSLMVGSLLETIFIT 330
Tm nAChR A ss: ECCHHHHHHHHHHHHHHHHHHHHHHHHHCC-HHHHHHHHHHHHHHHHHHHHHHHH----------HCC-CCCHHHHHHHHHHHHHHHHHH
Tm nAChR A ssPr: ECCCCEEHHHHHHHHHHHHHHHCEEECCCCCCCC-EEEEEEHHHHHHHHHHHHHHHHCCCCCCC----------CCH-HHHHHHHHHHHHHHHHEEEEEE
h5HT3A ssPr: ECCCHHHHHHHHHHHHHHHHHCEEECCCCCCC-EEEEEEHHHHHHHHHHHHHHCCCCCCCCC----------CCH-HHHHHHHHHHHHHHHHHEEEEE
h5HT3B ssPr: CCCCCHHHHHHHHHHHHHHHHCEEECCCCCCC-CEEEEEHHHHHHHHHHHHHHCCCCCCCCC----------CCH-HHHHHHHHHHHHHHHHHHEEE
h5HT3C ssPr: ECCCCEEEEHHHHHHHHHHHHHEEEECCCCCCC-EEEEEEEHHHHHHHHHHHHHHCCCCC--C----------CCH-HHHHHHHHHHHHHHHHHHHEE
h5HT3D ssPr: CCCCCEEEEHHHHHHHHHHHHHHEEECCCCCCC-EEEEEEEHHHHHHHHHHHHHHCCCCCCCCCCCCCCCCCCCCCCCCCCCHHHHHHHHHHHHHHHHHEEEEE
h5HT3E ssPr: EECCCEEEEEEHHHHHHHHHHHEEEECCCCCCC-EEEEEEHHHHHHHHHHHHHHCCCCCC--C----------CCH-HHHHHHHHHHHHHHHHHHEEEE
|---------TM1---------| |-----------TM2----------| |---------TM3--------
Tm nAChR A|298-437 NTHHRSPSTH < 307-374 > AIEGVKYIAEHMKSDEESSNAAEEWKYVAMVIDHILLCVFMLICIIGTVSVFAGRLIELSQEG--- 437
Tm nAChR B|303-469 NLHHRSPNTH < 313-403 > AVEAIKYIAEQLESASEFDDLKKDWQYVAMVADRLFLYIFITMCSIGTFSIFLDASHNVPPDNPFA 469
Tm nAChR C|311-484 NFHFRTPSTH < 321-421 > GIDSTNYIVKQIKEKNAYDEEVGNWNLVGQTIDRLSMFIITPVMVLGTIFIFVMGNFNRPPAK--- 484
Tm nAChR E|305-476 NVSLRTPNTH < 315-414 > CVEACNFIAKSTKEQNDSGSENENWVLIGKVIDKACFWIALLLFSLGTLAIFLTGHLNQVPE---- 476
ELIC|281-321 FAHHRQA--- < 289-293 > ----------DLLIQRCRLAFPLGFLAIGCVLVIRGITL--------- 321
h5HT3R A|328-478 RLVHKQDLQQ < 338-419 > LLQELSSIRQFLEKRDEIREVARDWLRVGSVLDKLLFHIYLLAVLAYSITLVMLWSIWQYA----- 478
h5HT3R B|325-441 KFLHDEQRGG < 335-380 > VWSQLQSISNYLQTQDQTDQQEAEWLVLLSRFDRLLFQSYLFMLGIYTITLCSLWALWGGV----- 441
h5HT3R C|331-447 YLLHVATTQP < 341-403 > ----------GWTKTQLMELWVQFSHAMDTLLFRLYLLFMASSILTVIVLWNT--------- 447
h5HT3R D|329-454 HLLHVATTQP < 339-402 > -----EWTRAQREHEAQKQHSVELWVQFSHAMDALLFRLYLLFMASSIITVICLWNT--------- 454
h5HT3R E|331-456 HLLHVATTQP < 341-404 > -----EWTRAQREHEAQKQHSVELWLQFSHAMDAMLFRLYLLFMASSIITVICLWNT--------- 456
Tm nAChR A ss: HHHHHCCCCC HHHHHHHHHHHHHHHHHHHHHHHHHCCCCCHHHHHHHHHHHHHHHHHHHHHHHHHHHHHC---
Tm nAChR A ssPr: EEEEECCCCC CHHHHHHHHHHHCCCCCCHHHHHCCEEEEEEEHHHHHHHHHHHHHHHHHHHHHCHHHHHHCCC---
h5HT3A ssPr: EEEECCCCCC CCHHHHHHHHHHHHHHHHHHHHHHHHHHHHHHHHHHHHHHHHHHHHHHHHHHHCCCCCCC-----
h5HT3B ssPr: EECCCCCCCC HHHHHHHHHHHHHHHHHHHHHHHHHHHHHHHHHHHHHHHHHHHHHHHHHHHHHHHCCCCC-----
h5HT3C ssPr: ECCCCCCCCC ----------HHHHHHHHHHHHHHHHHHHHHHHHHHHHHHHHHHHHEEEEEECC---------
h5HT3D ssPr: EECCCCCCCC -----HHHHHHHHHHHHHHHHHHHHHHHHHHHHHHHHHHHHHHHHHHHHEEEEEECC---------
h5HT3E ssPr: EECCCCCCCC -----HHHHHHHHHHHHHHHHHHHHHHHHHHHHHHHHHHHHHHHHHHHHEEEEEECC---------
---| |--------MA helix---------| |----------TM4-----------|

◀ **Fig. 1** Multiple sequence alignment between the structures of the four different subunits (A, B, C, E) of the nicotinic acetylcholine receptor from *Torpedo marmorata* (Tm nAChR; PDB code: 2BG9), the structure of a subunit of the pentameric ligand-gated ion channel from *E. chrysanthemi* (ELIC; PDB code: 2VL0) and the amino acid sequences of the five 5-HT_3R subunits A, B, C, D and E, manually adjusted on the basis of the ClustalW and structural alignments, and the prediction of the secondary structure. The prediction of the secondary structure (*ssPr*) is reported for the Tm nAChR A and for all the five human 5-HT_3 sequences: *C* = random structure; *H* = α-helix; *E* = β-strand. Moreover the secondary structure of the PDB structure of TM nAChR A is reported (*Tm nAChR A ss*). Transmembrane and intracellular regions are underlined (TM1, TM2, TM3, TM4, MA helix). The violet square contains the approximate TM1-TM2 linker and the TM2 region: within the alignment, the important residues for ion selectivity and gating (see Table 1) are highlighted with different colours: basic amino acids are blue, acidic are red, polar are orange and non-polar are green. The green square contains the MA-helix region in the IC domain: within the alignment, the important residues for ion conductivity (see Table 1) are highlighted with different colours: basic amino acids are blue, acidic are red, polar are orange and non-polar are green. Code: * = conserved residue in all sequences; : = different but highly conserved (very similar) residues;. = different residues that are somewhat similar

Nevertheless, recent works [27, 28] based both on modelling and experimental site-directed mutagenesis studies on the 5-HT_3R, demonstrated the requirements of at least one AA interface for any 5-HT_3R to be functional. To test this hypothesis, the 5-HT_3AB receptor, which is the most studied among the different heteropentamer, was also built considering all the other possible stoichiometries and arrangement (ABBBB, AABBB, AAABB, AAAAB, ABABA).

Briefly, the modelled structure of every subunit was superimposed to each of the five subunits of the TM and IC domains of the nAChR structure, to obtain a pentamer made of five identical subunits A or B or C or D or E. The heteromeric structures were built with the same procedure, superimposing either the modelled subunit A or one of the modelled subunits B, C, D, and E, onto each nAChR subunit in order to reproduce the desired arrangement.

Electrostatic potentials

The electrostatic potential of each pentamer was computed using the APBS software [54] through solution of the linear Poisson-Boltzmann (PB) equation, a continuum model for describing electrostatic interactions between molecular solutes in a salty and aqueous media. The PyMOL Molecular Graphics System, Version 1.2r3pre [55] was used as graphic interface for APBS (APBS Tools2.1) [56] and for the visualization of the resulting electrostatic potentials. The parameters used are: a grid dimension 137 × 136 × 163 $Å^3$ (which comprises the protein system of roughly 76 × 76 × 88 $Å^3$) with 161 × 161 × 193 grid points, Single Debye-Hückel sphere as boundary conditions, a ionic concentration of 0.150 M, a protein dielectric constant of 2 and a solvent dielectric constant of 78, a solvent radius of 1.4 Å and a system temperature of 310 K. Radii and charges were assigned using the web service PDB2PQR [57, 58], choosing the PARSE force field, optimized for implicit solvent calculations, before APBS calculations. The ± 1 kT/e electrostatic potential surfaces of each pentamer were plotted on the solvent-accessible surface.

Energy profile calculations

Electrostatics calculations based on the Poisson-Boltzmann (PB) equation provide an approximate evaluation of the energy profile of an ion passing through a channel [59].

PB calculations were performed using the software package APBS [54], to estimate the electrostatic contribution to the energy barrier for a calcium ion placed at successive points along the pore axis. The analysis of the pore was performed by means of the HOLE program [60] to obtain both the pore radius profile and the sample points along the pore axis to be probed by the Ca^{2+} ion. The web service PDB2PQR [57, 58] was used to assign radii and charges for all of the atoms, as previously described.

More precisely, the analysis of the pore performed by HOLE furnishes the coordinates of the pore axis: the pore axis lies parallel to the z-axis with coordinates (63, 63 Å, z), where z ranges between 50 and 110 Å. To have a detailed-enough description of the pore, the sample points where to place the Ca^{2+} ion were chosen to be 2 Å apart along the pore-axis, i.e. the sampled points were: P1 (63, 63, 50), P2 (63, 63, 52), P3 (63, 63, 54)…. P31 (63, 63, 110).

A cation with charge +2 and radius 1.86 Å, equivalent to the Born radius of calcium [61], was successively placed at each sample point. A single-point energy evaluation was performed and repeated for every of these sample positions, as described by Beckstein et al. [62]. Briefly, the grid dimensions containing the channel were 97 × 97 × 97 $Å^3$; a finer grid with dimension 10 × 10 × 10 $Å^3$ was used for focusing around the ion. The following parameters were used to simulate the environment: mobile ions Na^+ and Cl^- at a 0.150 M concentration; dielectric coefficients of 2.0 and 78 for the receptor and the solvent, respectively; temperature at 310 K. The electrostatic energy was calculated for three systems: $E_{protein}$, for the protein channel; $E_{ion}(z)$, for the ion by itself at each sample point z; $E_{complex}(z)$, for each protein-ion configuration (i.e. for each protein-ion complex with the ion at each sample point z). The PB energy at a sample point with coordinate z was then calculated, according to Tai et al. [63], as:

$$\Delta E_{PB}(z) = E_{complex}(z) - E_{ion}(z) - E_{protein} \quad (1)$$

For visualisation of structures VMD [64] was used.

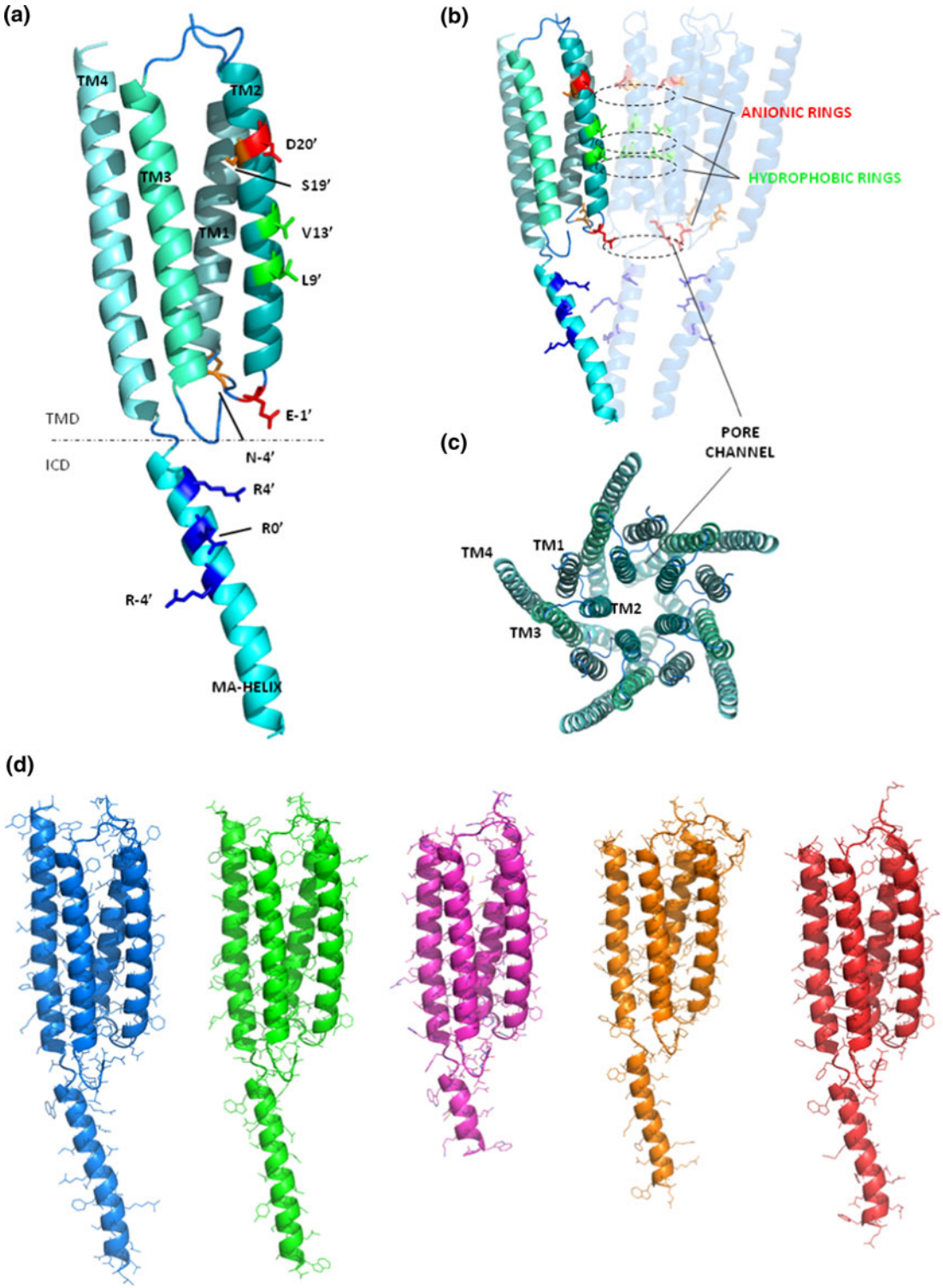

Fig. 2 **a** Homology model of the TM and IC domains of the 5-HT_{3A}R subunit. The important residues for ion selectivity, conductivity and gating [see Table 1] are shown in sticks and coloured according their physicochemical properties: basic amino acids are blue, acidic are red, polar are orange and non-polar are green. **b** Homology model of three of the five 5-HT_3A subunits that compose the pentamer receptor, showing how the highlighted residues are able to form anionic (D20′ and E-1′) or hydrophobic (L9′ and V13′) rings around the pore channel. **c** View of the homopentamer receptor 5-HT_3A from the extracellular side. The five subunits are assembled around a central channel pore and in each subunit the pore-lining domain consists of the TM2 transmembrane α-helix, while the TM1, TM3 and TM4 helices separate it from the membrane. **d** Homology models of the five 5-HT_3R subunit: A, B, C, D and E

Results and discussions

Modelling of the TM and IC domains of the 5-HT_3 A subunit

The model of the C-terminal part of the 5-HT_3A subunit is composed of four transmembrane α-helices (TM1, TM2, TM3 and TM4) and an intracellular α-helix (MA-helix). TM1 is connected to the EC domain and TM2 predominantly forms the wall of the channel pore (Fig. 2a). A short intracellular loop connects TM1 to TM2 and a short extracellular loop connects TM2 to TM3. TM3 and TM4 are connected by a long intracellular segment, which the MA-helix belongs to. This region, with the exception of the MA-helix, has not been modelled here because of the lack of its atomic coordinates in the nAChR template [4] (see Methods and Materials). The 5-HT_3A subunit structure model is shown in Fig. 2.

The selected 3D model appears to be a good starting point for further analysis, since its overall geometry, stereochemistry and packing are in compliance with the values typically observed in X-ray and NMR protein structures in the protein databases (see "Materials and Methods" and Online Resource) and it describes correctly the available experimental information [8]. In particular, experimental site-direct mutagenesis data demonstrate the determinant role played by a few residues located in the TM2 and MA-helices on biophysical properties such as single channel conductance, relative permeability, voltage-dependence, and desensitization (65–75). These are summarized in Table 1, where the spatial position of the residues in the model is also reported. The side chains of the residues directly involved in ion conduction and selectivity (E-1′, L9′, V13′, and D20′ in the TM2 helix, and R0′, R4′ in the MA helix) are directed towards the receptor pore (as clearly shown in Fig. 2a, b); the residues involved in voltage-dependence, and desensitization (K4′, L15′, I16′, and S19′ in the TM2 and R-4′ in the MA-helix) are mainly found in the inter-helices positions.

Sequence and structure comparison of the 5-HT_3 A-E subunits

The TM and IC domains of the receptor subunits B, C, D and E share with the A subunit a sequence identity of 44, 46, 39 and 48 %, respectively, therefore they could reasonably be modelled directly onto the 3D model of the 5-HT_3R subunit A. The analysis of the sequence alignment and of the structural models obtained (Figs. 1, 2d) showed that TM1, TM2 and TM3 are largely conserved within the 5-HT_3R subunits, while the TM4 is more variable. The major differences are in the loops connecting the α-helices;

Table 1 Single point mutations within the M2 and MA helices that affect the biophysical properties (single channel conductance, relative permeability, voltage-dependence, desensitization) of the 5-HT_3A receptor

Residue affecting function	Mutation(s)	Position	Function involved	References
E-1′	A	TM2 pore	Ion selectivity, alone or combined with V13′T or S19′R	[65–67]
K4′	R/Q/S/Q/G	TM2 inter-helix	Increase desensitization	[68]
L9′	F, Y, A, C	TM2 pore	Channel gate; affect desensitization	[69]
V13′	S, T	TM2 pore	Channel gate; ion selectivity when combined with E-1′A	[65, 70]
L15′	C	TM2 inter-helix	Standing current	[69]
I16′	T/C	TM2 inter-helix	T: increase desensitization; C: standing current	[69, 71]
S19′	R	TM2 inter-helix	Increase desensitization; Ion selectivity when combined with E-1′A	[66]
D20′	A	TM2 pore	Ion selectivity (reduced Ca^{2+} permeability)	[72]
R-4′	Q	MA-helix	Single channel conductance when combined with R0′D and R4′A	[73, 74]
R0′	D, E, Q, F, C	MA-helix	Single channel conductance, alone or combined with R-4′Q and R4′A	[73–75]
R4′	A	MA-helix	Single channel conductance, alone or combined with R0′D and R-4′Q	[73, 74]

in particular, the TM2-TM3 loop in subunit D is much longer than the corresponding loop in the other subunits. It protrudes towards the extracellular portion of the receptor, where the long N-terminal domain (not included here) is found. In addition, the MA-helix in subunit C is shorter than MA-helices in the other subunits.

The modelled subunits A to E were combined to build 3D models of the 5-HT_3R TM and IC domains with different stoichiometries: (1) homopentameric 5-HT_3R A, B, C, D and E; (2) heteropentameric 5-HT_3R A/B with stoichometries AAAAB, AAABB, AABBB, ABBBB, ABABA, BBABA; (3) heteropentameric 5-HT_3R A/C, A/D, A/E with stoichiometry analogous to the BBABA (i.e. CCACA, DDADA, EEAEA).

The analysis of all these receptor models revealed that the intra- and inter-subunit interactions found are very similar among the different subunits. For example, a carbon-π network is established between few residues of TM1 and TM4 helices and is conserved in all the subunits (F264-I457, Y458-I261, Y265-L454 [sub. A numeration]; see Fig. 3a); moreover, an inter-subunit carbon-π connects F14′ (conserved in all the subunits) from TM2 to either I16′ (A subunit), V16′ (B subunit) or L16′ (C, D and E subunits) from TM2 of the adjacent subunit (Fig. 3b), which means that the same interaction is present between all subunit interfaces (AA, AB, BA, BB, AC, CC, CA, AD, etc.…).

As for the relevant residues in Table 1, those at TM2 position 20′, -1′ and -4′ were mutated in the nAChR [76, 77] and were demonstrated to form three rings of residues along the pore that act as determinants of ion conduction in cation selective channel. The residues at positions 20′ and −1′, which are conserved in the 5-HT_3A subunit (Fig. 1), were shown to be determinant also in the 5-HT_3R. Gunthorpe and Lummis [65, 66] neutralized the intermediate ring of residues, inserted a Pro between the −1′ and −2′ residues and replaced the 13′ Val by a Thr, transforming the cation permeable receptor into an anion permeable receptor. However, the single mutation of the E-1′A was proved to cause the channel to be non-selective [78]: this is a clear indication of the importance of this residue in controlling ion selectivity. Interestingly, this mutation is naturally present in the B subunit (the residue at position −1′ is an Ala, instead of the Glu found in the A subunit; see Fig. 1). This suggests that if the homomeric 5-HT_{3B}R was formed (as reported by Holbrook et al. [24], who observed the expression but not the function of the homomeric 5-HT_{3B}R), it would not be ion selective. In subunit C, D and E the residue at position -1′ is an Asn (Fig. 1), which although not being charged,

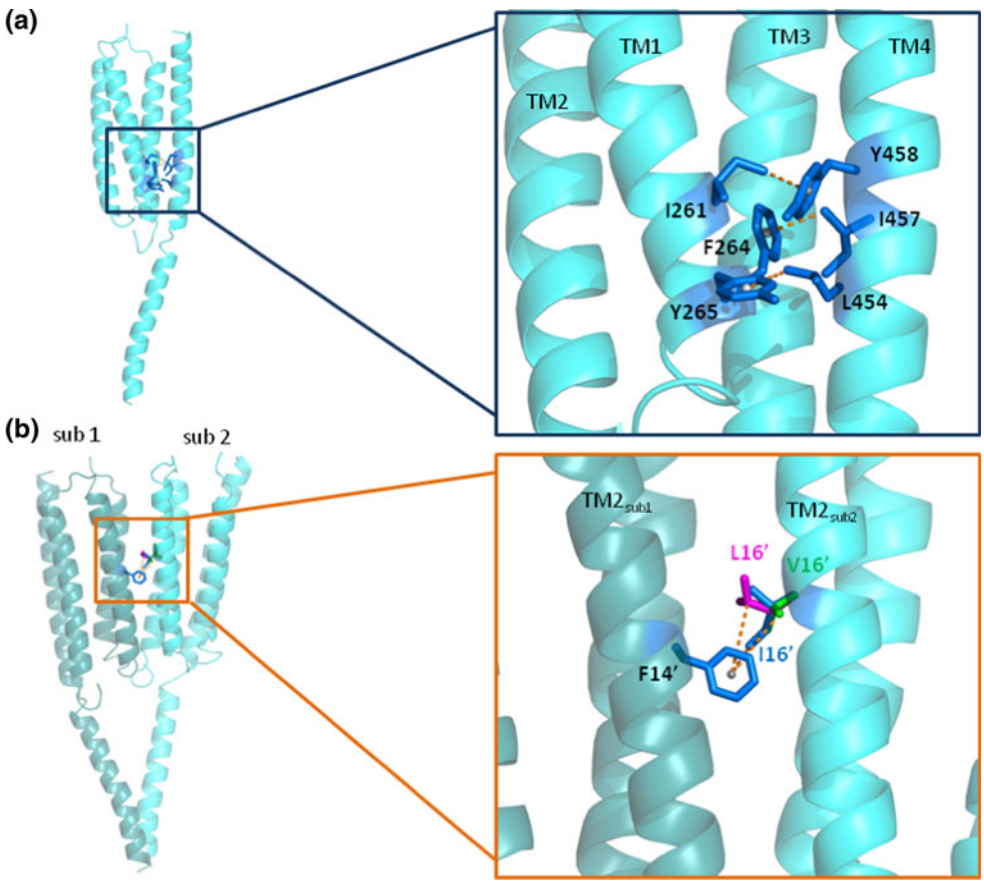

Fig. 3 **a** Homology model of the 5-HT_{3A}R subunit showing the intra-subunit carbon-π network connecting some residues of the TM1 and TM4 helices. This is conserved in all the subunits [F264-I457, Y458-I261, Y265-L454 (sub. A numeration)]. **b** Homology model of a dimer of the 5-HT_{3A}R showing the inter-subunit carbon-π that connects F14′ (conserved in all the subunit, identified as sub 1) in TM2 to either I16′ (*blue*, A subunit), V16′ (*green*, B subunit) or L16′ (*pink*, C, D and E subunits) in the TM2 of the adjacent subunit (sub 2)

maintains the local physicochemical properties of subunit A, thanks to its polarity.

The negative ring formed by aspartic acids in position 20′ is conserved in all the subunits except the B subunit, where this position is occupied by an Asn (Fig. 1), which is nevertheless polar. The absence of an acidic residue at the outer ring position of the β2 subunit of the nAChR has been demonstrated to cause a reduction in Ca^{2+} permeability [79], as well as it happens in the heteromeric 5-HT_{3AB}R [80].

As for residue at TM2 position -4′, instead, sequences analysis pointed out that the properties of this residue, which is an Asp in nAChR α subunit, are conserved only in subunits C and D, where a Glu is present, while in the subunits A and B there is a polar residue (Asn), and in subunit E a positive one (Lys) (Fig. 1). This variability causes the local properties of the different subunits to be largely diverse for the different 5-HT_3R subunits and suggests that the role of this residue might not be primary in the 5-HT_3 receptors. This hypothesis is supported by the fact that: (1) in analogy to the 3D structure of the nAChR, this residue is not protruding into the channel pore cavity of any of the modelled 5-HT_3Rs; (2) this residue has never been mutated in the 5-HT_3Rs, therefore its direct involvement in ion selectivity in the 5-HT_3R has not been directly ascertained, yet.

The key residues important for the conductivity (see Table 1) are those at the MA −4′, 0′ and 4′ positions. In the 5-HT_3A subunit, these three residues, which lie at the boundary with the cytoplasmic region, are Arg. Site-directed mutagenesis experiments showed that replacement of these three Arg, and in particular of R0′, causes a large increase in channel conductance [72, 74]. These findings arose from the observation that the incorporation of the 5-HT_3B subunit (where no Arg is present at the key positions −4′, 0′, 4′; see Fig. 1) into the receptor to form the heteromeric 5-HT_3AB receptor makes the conductance increase, changing from values in the femtosiemens range (for the homomeric 5-HT_{3A}R) to picosiemens (for the heteromeric 5-HT_{3AB}R) [80]. The role played by R-4′, R0′ and R4′ in modulating the receptor conductivity was confirmed also for the nACh α4β2 receptors, where the replacement of the natural residues at the MA −4′ and 0′ positions with Arg caused significant reduction of the single channel conductance [74]. Interestingly, in none of the other 5-HT_3R subunits (i.e. B, C, D and E) Arg residues are present at these sequence positions within the MA-helix, which are instead occupied by polar, negative or apolar residues: Q-4′, D0′, A4′ in the B subunit; G-4′, T0′, E4′ in the C subunit; E-4′, Q0′, E4′ in the D and E subunits (see sequence alignment in Fig. 1). This leads to the hypothesis that, by similarity with the 5-HT_3AB receptor, the conductivity of the heteropentamers 5-HT_3AC, 5-HT_3AD and 5-HT_3AE, might be larger than that of the homomeric 5-HT_{3A}R (note that single channel conductance for 5-HT_3AC, 5-HT_3AD and 5-HT_3AE heteromeric receptor has not been reported yet) [81]. In contrast to the work of Holbrook et al. [24], where the alignment of the five 5-HT_3 subunit sequences showed a disruption of the 5-HT_3C MA-helix with residues at 0′ and 4′ positions not being represented, here the 5-HT_3C subunit model was built under the hypotheses that the MA-helix in the C subunit is shorter than in the other subunits, and that the key residues R-4′, R0′ and R4′ in the 5-HT_3A are replaced respectively by Gly, Thr, and Glu (Fig. 1).

Finally, residues L9′ and V13′ in TM2 (A subunit), are supposed to be involved in the gate mechanism [69]. In fact, experimental studies clearly demonstrated that the conserved L9′ in TM2 domain play an important role in gating: substitution of this amino acid with the more polar amino acid Thr affects the rate of desensitization and the EC_{50} for the activation of both the AChR and 5-HT_3R [21, 67]. In addition, the substitution of V13′ with a serine produces spontaneous gating in 5-HT_3R [70]. L9′ and V13′ are highly conserved among the 5-HT_3R subunits, the only exception being subunit B, where the conservative substitution L9′V is observed; thus, apparently, all the receptors studied should have the same gating mechanism.

Electrostatic potential surface

The physico-chemical characterization of the TM and IC 5-HT_3R domains is an interesting starting point to understand the determinants of ion conduction of the several pentamers constituting the 5-HT_3R family.

The electrostatic and hydrophobic properties of the EC domain of subunits 5-HT_3 A and B were published in a previous paper [34]. The analysis of the results showed that, while long range forces favour the formation of EC AA and BA dimers with respect to formation of dimers AB and BB, at short range the AB interface is favoured. This led to hypothesize that, on electrostatic bases, besides the assembling of the homopentamer A, which is probably quite fast, assembling of the ABABA and the BBABA pentamers are equally probable, while assembling of the BBBAA structure is less favoured. Moreover, the interfaces AA and AB showed to be very similar in the capability to bind ligands (both serotonin and antagonists), while the BA interface, similarly to the interface BB was supposed to be unable to bind ligands; following the same line of reasoning and taking into account also subunits C, D and E, only the CA and EA interfaces were predicted to be able to bind ligands in functional receptors.

In the present study the surface of the pore and of the portals through which the ions exit and enter the vestibule has been investigated by means of the molecular electrostatic

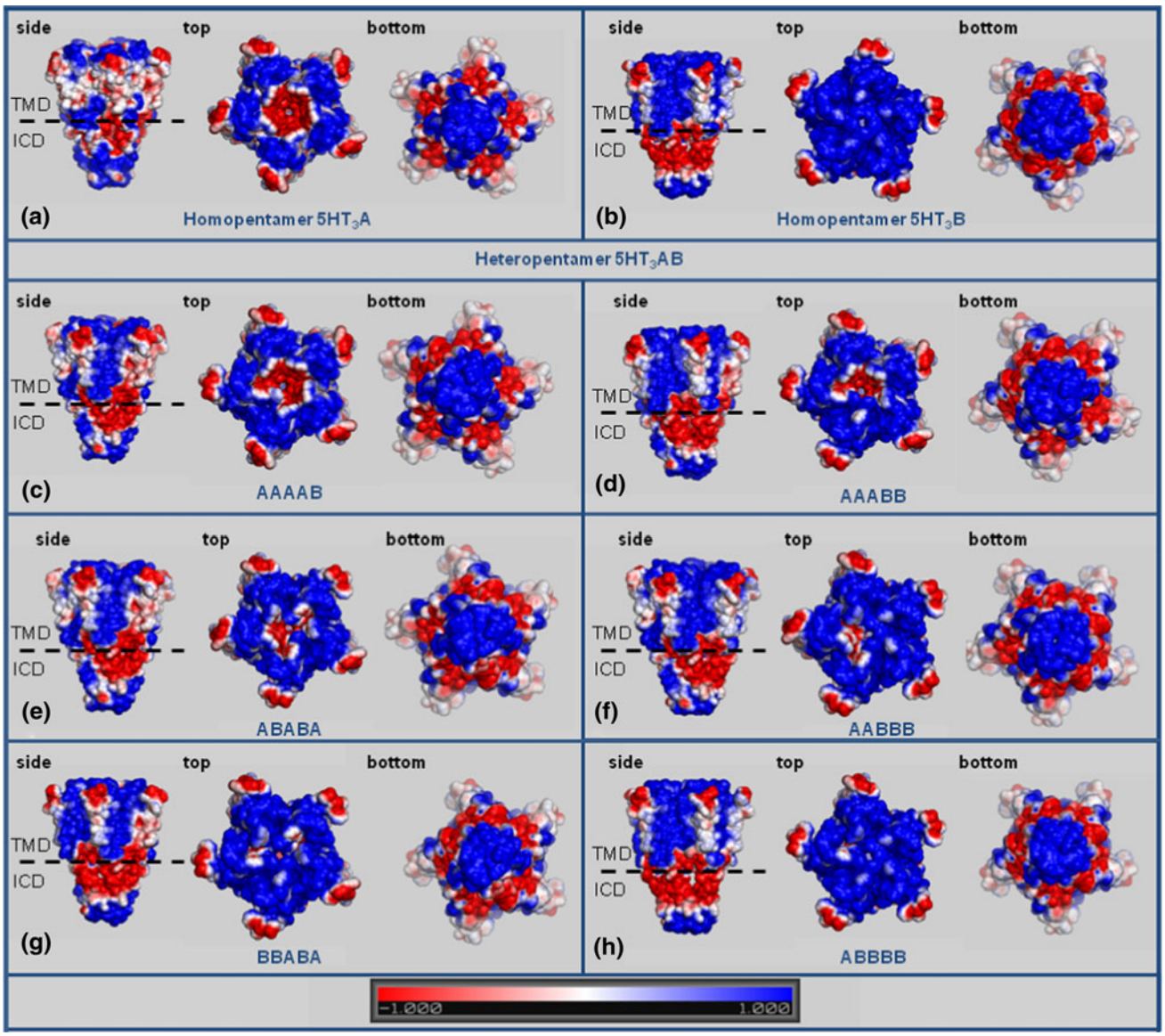

Fig. 4 Electrostatic properties of the homomeric and heteromeric 5-HT_3A, 5-HT_3B and 5-HT_3AB receptors. MEPs isocontour levels are shown at +1 kT/e (*blue*) and -1 kT/e (red). **a** Representation of MEP isocountour levels of the side, *top* and *bottom* view of homopentamer 5-HT_3A; **b** Representation of MEP isocountour levels of the side, top and bottom view of homopentamer 5-HT_3B; **c**–**h** Representation of MEP isocountour levels of the side, *top* and *bottom* view of all the stoichiometries of heteropentamer 5-HT_3AB

potential (MEP) only. In fact, vdW forces are expected to play a role mainly in the packing of the TM helices and in the dynamics of the transition between the different states of the receptor (resting, open, closed); this is not the focus of the present study which aims at giving a static picture of the modulation of the determinants of ion conduction by the stoichiometry and arrangement of the different subunits.

The MEP isocontour levels are represented in Figs. 4 and 6. The analysis of the electrostatic features was performed for the homopentameric receptors 5-HT3A, 5-HT3B, 5-HT3C, 5-HT3D and 5-HT3E and for the heteropentameric receptors 5-HT3AB, 5-HT3AC, 5-HT3AD and 5-HT3AE with stoichiometry XXAXA (where X is subunits B, C, D or E). Only for the most studied heteropentamer, the 5-HT3AB receptor, all the other possible stoichiometries were also considered (ABBBB, AABBB, AAABB, AAAAB, ABABA).

The electrostatic potential map of 5HT$_3$A homopentamer receptor surface

The first evident feature shown by the TM and IC domains of the homopentamer 5-HT_{3A}R is the overall negative electrostatic potential inside the pore (Fig. 4a, and Online Resource Fig. 1). Smaller regions of positive potential characterize the upper region of the TM domain, where the

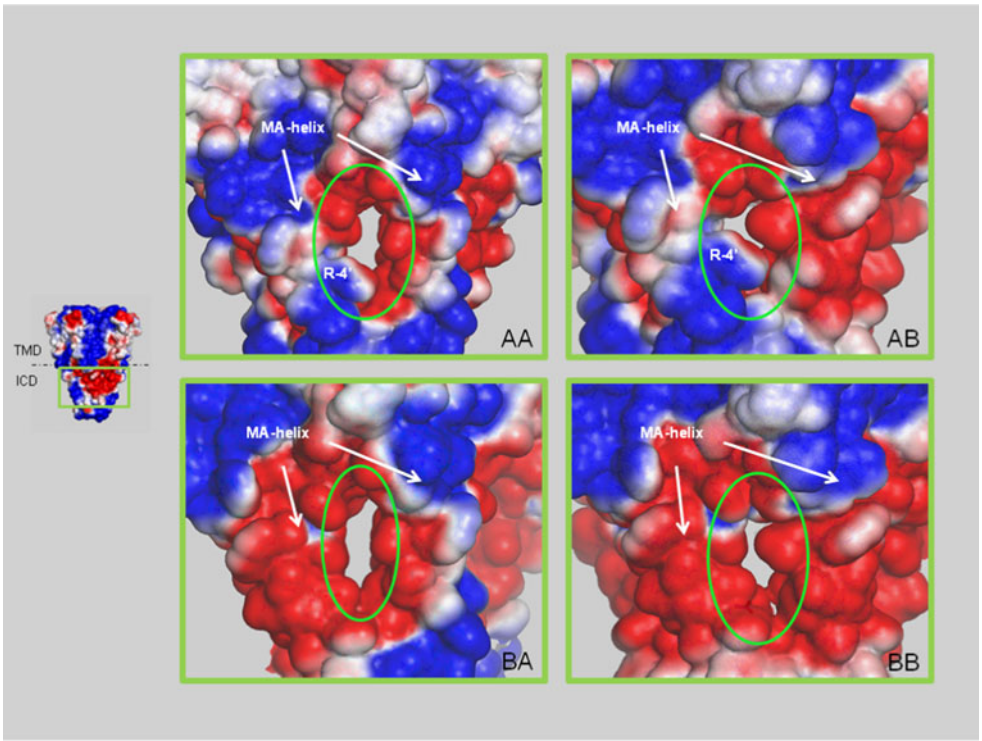

Fig. 5 Electrostatic properties of the portals in the 5-HT_{3AB}Rs IC domain, putative way out of ions. MEPs isocontour levels of exterior views of the IC domain section are shown at +1 kT/e (*blue*) and −1 kT/e (*red*) for AA, AB, BA and BB portals, formed between two adjacent MA-helices

EC domain is located (Fig. 4a). To this respect, the electrostatic potential of the region at the boundary between the EC and the TM domains might suffer from the fact that the EC domain is not included in the models. Examination of the pore model structure of 5-HT_{3A}R showed that the majority of the TM2 residues forming the pore are negatively charged or at least polar residues, such as Asp, Glu, Thr or Ser, which confer to the pore its negative potential. The portion of the IC domain closer to the membrane is also characterised by a negative potential (see Fig. 4a), despite the presence of three Arg (R-4′, R0′,R4′) in the amino acid sequence (see Figs. 1, 2a).

The large negative potential along the TM channel and part of the IC channel is likely to play a significant role in the interaction of the receptor with ions. In fact, previous studies demonstrated that there is a very high barrier for an ion moving inside a low dielectric environment [82, 83], suggesting, therefore, that ion channels (which represent a low dielectric environment) need charged surfaces, or at least partial charged surfaces, in order to allow ions to enter. This hypothesis was subsequently investigated and confirmed by Kuyucak et al. [84], who analysed the interaction of ions with a simple geometry channel.

On the contrary, the C-terminus of the IC domain (i.e. the region more distant from the membrane) is characterised by a large area of positive potential that, on simple electrostatic consideration, repels the fluxed cations, promoting their exit through the lateral openings (portals) found in the receptor IC domain (Fig. 4a).

These portals are formed at the interface of two adjacent MA-helices and are therefore, in principle, five. Interestingly, they show surface electrostatic potential that is overall negative and could in fact attract the fluxed cations. The presence of highly charged portals, through which ions go out of the channel, was previously suggested by Mokrab et al. [85] for the GABA receptor, which is anion-selective; in that work, the interaction energy between a Cl^- ion and the GABA model structure was calculated along the central pore of both the EC and TM domain, and along the putative exit paths in the IC domain through each of the five portals, to determine the most favourable energy profiles.

The portals in the 5-HT_3A homopentamer are not completely negatively charged (see Fig. 5) and show instead local areas of positive potential. The presence of these positive spots could slow down the movement of cations though the portals and thus explain the lower single channel conductance observed for the homopentamer A with respect to the heteropentamer AB. [26] The positive areas inside the portals are due to the three non conserved Arg located in the TM2 (R-4′, R0′,R4′) [74], whose role has been discussed in a previous paragraph.

The electrostatic potential map of 5HT_3B homopentamer receptor surface

The electrostatic potential map of 5HT_3B homopentamer receptor surface reveals in part opposite characteristics with respect to those of the 5HT_3A homopentameric

receptor. The TM domain of the $5HT_3B$ homopentameric receptor has a positive MEP, both inside the pore and outside, with very small regions of negative potential in the external part of the receptor, near the EC domain (Fig. 4b). On the contrary, with the exception of the positive potential of the MA-helix N-terminus (which lies far from the membrane), the IC domain is characterised by an overall large negative electrostatic potential.

Interestingly, the MEP that characterises the TM domain channel in the homopentameric $5HT_{3B}R$, is highly positive, despite the low number of positive residues in the TM2 sequence (Fig. 1). This is due to the fact that the two important negative residues E-1′ and D20′ which were found in the A subunit TM2, are substituted in the B subunit by non-charged residues (i.e. E-1′A and D20′N). This is a further confirmation of the role played in ion selectivity of the two charged rings formed by these residues in the TM2 helix bundle of the receptor (−1′ and 20′; see Modelling section) [65, 66].

The electrostatic potential map of heteropentameric 5-HT$_3$AB receptor surface

Surprisingly, the potential surface map of the heteropentameric 5-HT_3AB receptor, with the stoichiometry BBABA proposed by Barrera et al. [26], exhibits the same qualitative electrostatic characteristics of the homopentamer 5-$HT_{3B}R$, i.e. a positive pore surface in the TM domain, a negative surface at the entrance of the ICD (near the membrane), and a positive region at the N-terminus of the MA-helices (Fig. 4g). Such a MEP similarity suggests that also the heteromeric BBABA receptor could be non functional, similarly to the homomeric B pentamer. In addition, in the heteromeric receptor BBABA, the MEP characteristics of the B subunit seem to prevail on those of the A subunit, masking the negative potential areas of the TM2 domain. Similarly, the analysis of the MEPs of the heteropentameric 5-$HT_{3AB}R$ with other stoichiometries such as AABBB, or ABBBB, shows that the presence of three or more B subunits confers to the pore a positive potential that could disadvantage or block the cations passage (Fig. 4f, h), due to electrostatic repulsion. However, it is worth noting that, as it has been showed in previous studies [34], the MEP of the BBABA EC portion is highly negative, and therefore seems to be favourable to cation permeation. The fact that the pore has opposite electrostatic features in the EC and TM domains might have relevant implications for the effective functionalities of the 5-HT_3R with this stoichiometry: it can not be excluded that this receptor is functional notwithstanding the detrimental electrostatic potential of the TM domain pore.

On the contrary, in pentamers with stoichiometry 2B:3A and 1B:4A (i.e. AAAAB, AAABB or ABABA), the pore potential surface is mainly negative (Fig. 4c–e), as in the all-A receptor. Of course, in 2B:3A 5-HT_3Rs, there are small positive MEP regions at TM domain facing the EC domain, which are found where subunits B are located. However, these seem not to influence the whole pore surfaces, which results favourable to cations passage. Interestingly, the MEP of the pore in the EC portion of the ABABA receptor is negative [34], thus the whole receptor pore (the EC, the TM and the C-terminal IC domains pore) is completely negative, with the only exception of the MA-helix N-terminus (Fig. 4e). Therefore, on simple electrostatic bases, of all the possible receptor stoichiometry considered here, the one which seems to be fully functional is the heteropentamer ABABA, followed by the homomeric A, although also for the heteromeric BBABA functionality cannot be excluded.

Despite the fact that the pore potential surfaces of the TM domain differ depending on the number of the B subunits present in the pentamer, the MEP surfaces of the IC domain is always negative, with only a small positive region found at the N-terminus of the MA-helix, which may reasonably repels positive charges, such as cations, thus limiting or blocking their movements across the channel.

The IC domain of the various receptors differ mainly in the region of the portals formed between two adjacent MA-helices; in fact, portals formed by different subunit couples (AA, AB, BA, BB) show different dimensions and potentials (Fig. 5). More precisely, the BB and BA portals are the largest and their MEP is completely negative; the AA portal is smaller than the BB and BA portals and has a positive MEP region due to the presence of R-4′, R0′ and R4′ in the A subunit; the AB portal is the smallest and has a MEP distribution which is similar to that of the homopentamer A portal. The different features of the portals could influence the ion exit in different manners, increasing the single channel conductance when at least one B subunit is present, in agreement with the experimental data [74].

In summary, the heteropentamer 5-$HT_{3AB}R$ with BBABA stoichiometry [26] shows a positive MEP of the TM domain portion of the pore detrimental for the cations passage, although the highly negative MEP of the EC portion of the pore [34] would promote it. The receptor stoichiometries that have a negative TM domain pore potential surface favourable for cation flux are AAABB, AAAAB and ABABA. These results seem to support the hypothesis by Lochner and Lummis [27] according to which the BBABA stoichiometry is not functional, because it lacks the minimum requirements of an interface AA. However, as previously explained, also the BBABA receptor might be somewhat functional, as a consequence of flux modulation due to the interplay between the physicochemical features of its EC [34] and TM domains.

In conclusion, from the analysis of the electrostatic potential properties of the pore surface of homopentameric and heteropentameric 5-HT_3 A/B receptors performed in this work, the requirement of having at least one AA interface is not sufficient for the receptor to be functional. Instead the requirement for receptor functionality is a maximum of two B subunits. In fact, the pentamer AABBB, containing one AA interface, presents a positive surface along the TM pore which may prevent or limit the cations passage.

The electrostatic potential map of other homo- and heteropentameric receptor surfaces

For 5-HT_3R subunits C, D and E, only the homopentamers and the heteropentamers with stoichiometry similar to that experimentally found for the AB receptor [26] (CCACA, DDADA, EEAEA) were taken into account here. Figure 6 (*left*) shows the potential map surfaces of the homopentamers 5-HT_3C, 5-HT_3D and 5-HT_3E receptors which exhibit very similar characteristics to the homopentamer 5-HT_3A receptor. In fact, the pore surface is characterized in all cases by a negative MEP, extending from the TM domain near the EC domain until the centre of the MA-helix in the IC domain, while the IC domain C-terminus is on the contrary is positive.

There is still an open debate on the expression of the homopentamer 5-HT_3C, 5-HT_3D and 5-HT_3E receptors: Nielser et al. [23] showed that subunits C, D and E do not reach the plasma membrane unless co-expressed with the A subunit, while Holbrook et al. [24] suggested that these subunits can independently reach the plasma membrane. However, both the studies agree on the non-functionality of these three homopentamers. Considering the results obtained in this work, it is not possible to find a reasonable explanation to their lack of functionality, which is probably due to factors diverse from those analysed here.

The potential surface maps of the heteropentameric 5-HT_3AC, 5-HT_3AD and 5-HT_3AE receptors are not different from those of the corresponding homopentameric receptors: a negative MEP prevails along the pore (Fig. 6 *right*), which might attract cations and promote their passage and force them to exit through the large and negative portals in the IC domain. The single channel conductance,

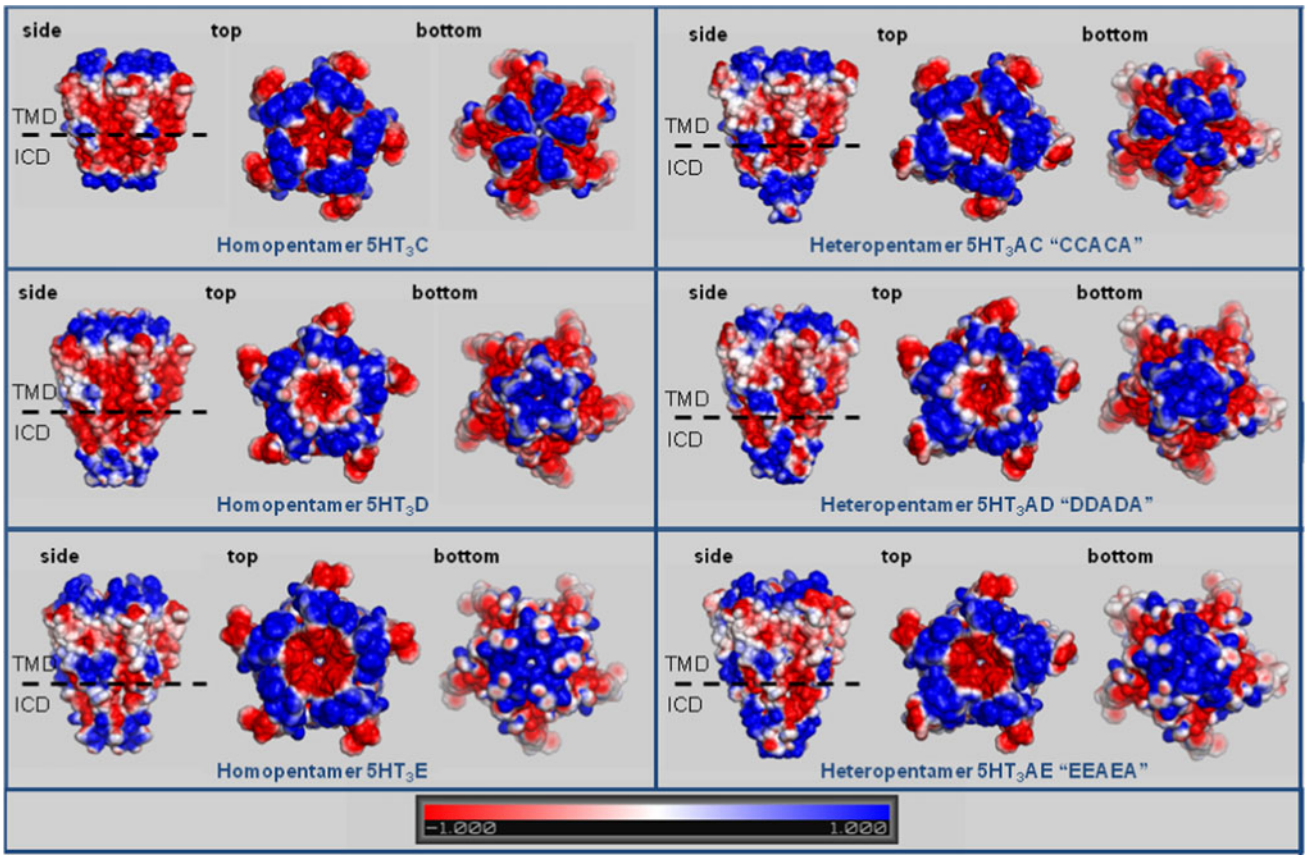

Fig. 6 Electrostatic properties of the homomeric 5-HT_3C, 5-HT_3D, 5-HT_3E and heteromeric 5-HT_3AC, 5-HT_3AD, 5-HT_3AE receptors. MEPs isocontour levels are shown at +1 kT/e (*blue*) and −1 kT/e (*red*). *Left*: Representation of MEP isocountour levels of the side, *top* and *bottom* view of homopentamers 5-HT_3C (*top*), 5-HT_3D (*middle*) and 5-HT_3E (*bottom*); *right*: Representation of MEP isocountour levels of the side, *top* and *bottom* view of heteropentamers 5-HT_3AC (*top*), 5-HT_3AD (*middle*) and 5-HT_3AE (*bottom*)

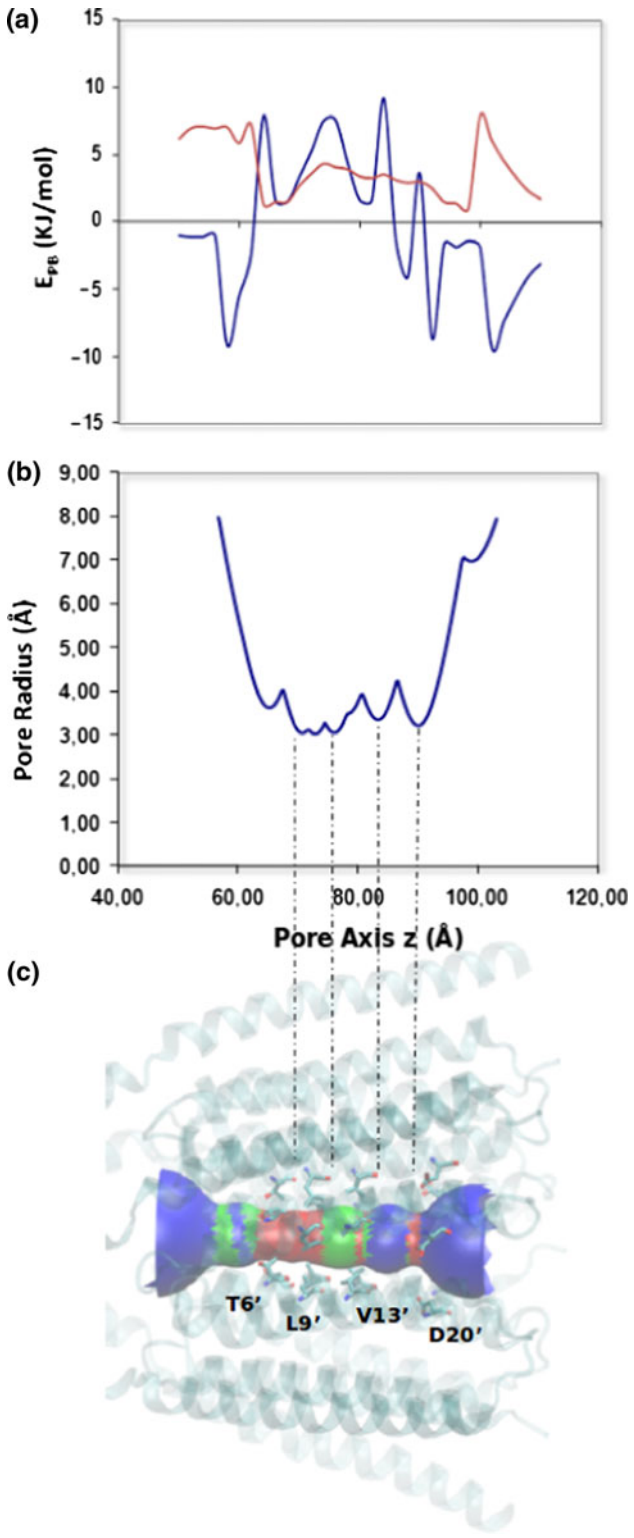

◀**Fig. 7** **a** PB energy profiles for a calcium (*blue line*) and a chloride (*red line*) ion encountering the 5-HT_{3A}R pore; **b** pore radius profile for the 5-HT_{3A}R pore; **c** model of the 5-HT_{3A}R oriented such that the pore (*z*) axis coincides with that of the graphs **a** and **b** (to the *left* is the IC domain, *right*, the EC domain; neither shown). The *solid* surface in **c** represents the pore lining surface, calculated using HOLE [60] and coloured on the basis of the radius pore as follows: R < 3.5 Å red, 3.5 Å < R > 4 Å green, R > 4 Å blue. Residues of interest, corresponding to the constrictions of the pore lining surface, are shown in sticks. Note that these residues match to the minima in the pore radius pore (**b**) and to the peaks on the calcium ion PB energy profile (**a**)

which has not been experimentally measured yet [81], should be greater in the heteropentameric 5-HT_3AC, 5-HT_3AD and 5-HT_3AE receptors than in the homopentamer 5-HT_{3A}R. However, further hypotheses about the putative stoichiometry of these three heteropentamers cannot be developed on simple electrostatic characteristics, since their MEPs are highly similar to that of the homopentamer 5-HT_{3A}R.

Pore profile

On the basis of the results obtained by the MEP analysis, the homopentameric and heteropentameric receptors built by subunit A and B were selected for a detailed characterization of the physicochemical properties of their pores.

It is important to remember that these three-dimensional models correspond to a closed state of the channel, because the structure of the templates was obtained in absence of the agonist.

Analysis of the 5-HT_{3A}R pore radius profile (Fig. 7b) showed that there are some constrictions along the length of the pore, which extends along the z axis, from z 56 Å (TM domain portion at the IC boundary) to z 103 Å (TM domain portion at the EC boundary). At the smallest section of the channel, which is in the proximity of the TM2 T6′ ring and of the hypothesized gate channel formed by L9′ and V13′ [67, 69, 70], the channel radius is about 3 Å; another narrowing, where the channel radius is about 3.5 Å, is in the nearby of the TM2 D20′ ring of residues, which is important for the ion selectivity [65, 66], as previously discussed. These results are consistent with those obtained for the nACh receptor in previous studies [86], where it was suggested that the conserved rings of L9′ and V13′ do not form a physical block in this region, but constitute an ion-impermeable hydrophobic barrier [14]. More in detail, Beckstein et al. [87] explained that a hydrophobic gate acts as a desolvation barrier for ions, in fact the narrow pore radius (R < 4 Å) forces ions to shed at least some water molecules from their hydration shell, which requires a large amount of energy, in order to pass the constriction.

In addition to the pore radius profile, the energetic profile of a calcium ion, as it translates along the pore axis, has been estimated by means of Poisson-Boltzmann energy calculation. This method has some intrinsic limitations such as: static protein structures are considered, and only the long-range electrostatic forces are calculated; therefore, the non-electrostatic effects and those due to movements of

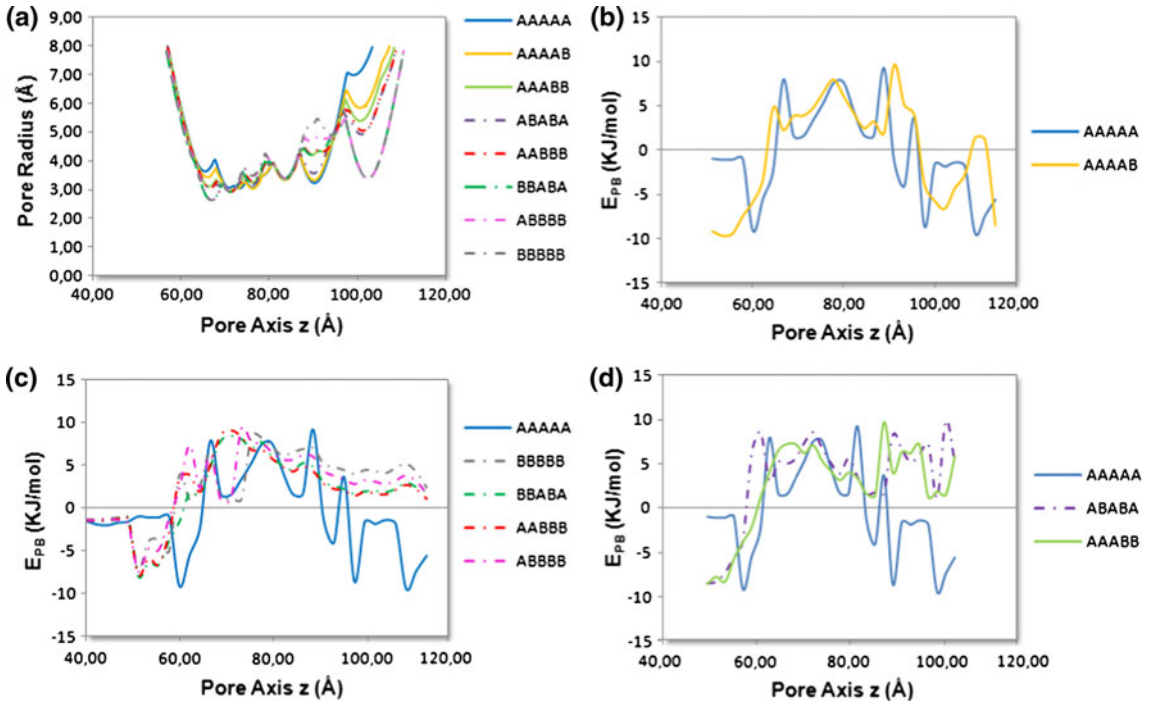

Fig. 8 Pore radius profiles (**a**) and calcium ion PB energy profiles (**b**, **c**, **d**) for homomeric and heteromeric 5-HT$_3$A, 5-HT$_3$B and 5-HT$_3$AB receptors: 5-HT$_{3A}$R "AAAAA" in *blue*, 5-HT$_{3B}$R "BBBBB" in *grey* (*dashed line*), 5-HT$_{3AB}$R "AAAAB" in *yellow*, 5-HT$_{3AB}$R "AAABB" in *green*, 5-HT$_{3AB}$R "ABABA" in *purple* (*dashed line*), 5-HT$_{3AB}$R "AABBB" in *red* (*dashed line*), 5-HT$_{3AB}$R "BBABA" in deep *green* (*dashed line*), 5-HT$_{3AB}$R "ABBBB" in *pink* (*dashed line*)

the pore-lining residues are not considered. To include these effects, energy profiles could be computed by potential mean force (PMF) calculations, which are based on molecular dynamics. These calculations would be more accurate, but at the same time much more time-expensive. Previous theoretical studies demonstrated that, notwithstanding PB calculations commonly overestimate the barrier for narrow (<3 Å) channels with respect to PMF calculations [62], the two methods reach the same conclusions on the α7 nicotinic receptor model [86].

Figure 7a shows the PB energy profile of a calcium ion approaching the 5-HT$_{3A}$R channel from the extracellular domain (right). The negative potential that characterizes the pore (see Electrostatic potential surface section) exerts a favourable attraction in the region located between 120 and 90 Å in the z direction. The small energy barrier at z 90 Å is due to the bottleneck corresponding to D20′ residue, and the larger energy barrier at the centre of the pore extends from the V13′ through the L9′ to the T6′ side chain rings. Consistently with the closed state 3D model used, this energy barrier provides a significant block to permeation. Finally, at the end of the TM domain, towards the IC domain, the PB energy becomes negative again.

These results are consistent with those obtained for the nACh receptor [14, 86] and with the hypothesis of a hydrophobic gate, formed by a hydrophobic region in the centre of the pore [69] that plays a role as a barrier to ion permeation in the closed receptor conformation. This energy barrier is lowered upon ligand binding by asymmetric movement of M2 helices that increases the diameter of the pore near the middle of the membrane by about 1Å [16].

For comparison, the PB energy profile of the anion Cl^- ion has also been calculated. The energy profile showed in Fig. 7a reveals a totally non favourable permeation of this ion through the 5-HT$_{3A}$R pore. In particular, chloride ions encounter a high barrier (7 Å) already at the channel entrance. This repulsion is probably caused by the Asp in TM2 position 20′ (whose structural position corresponds to the peak barrier). This demonstrates that the presence of this negative residue at the TM channel entrance, together with the whole negative pore MEP in the TM domain, contributes to the ion selectivity of the channel.

The pore radius and the PB energy profiles of the homopentamer 5-HT$_{3B}$R and of the various stoichiometries of the heteropentamer 5-HT$_{3AB}$Rs were analysed and compared to those of the homopentamer 5-HT$_{3A}$R. The pore radius profiles (Fig. 8a) show similar trends at the level of the channel gate (V13′, L9′) and of the T6′ residue ring, while the main differences with the homopentamer 5-HT$_{3A}$R are located in three principal regions:

- at z 101 Å, where in the A subunit is present an Ala, whereas in the B subunit there is a bulkier Arg. There,

the radius decreases with the increasing of the number of B subunits present in the receptor (i.e. radius 5-HT_{3A}R = 7 Å vs. radius 5-HT_{3B}R = 3.5 Å), and, in case the number of B subunits in the receptor is the same, the local channel radius is smaller where B subunits are not adjacent;

- at z 90 Å, where in the B subunit is present an Asn instead of the Asp of the A subunit. There, the radius increases with the increasing of the number of B subunits present in the receptor (i.e. radius 5-HT_{3A}R = 3.5 Å vs. radius 5-HT_{3B}R = 5.3 Å);
- at z 65 Å, where in the B subunit is present an Ile instead of the Val of the A subunit. There, the radius decreases with the increasing of the number of B subunits present in the receptor (i.e. radius 5-HT_{3A}R = 4 Å vs. radius 5-HT_{3B}R = 2.7 Å).

Analysing the trend of the PB energies of the homopentamer 5-HT_{3B}R and of the heteropentamer 5-HT_{3AB}Rs, it is possible to distinguish three different profile types. The first type is that of the "AAAAB" heteropentamer, which is very similar to that of the homopentamer 5-HT_{3A}R (Fig. 8b), characterised by the same peak in correspondence of the channel gate. The only difference is a small peak (1.20 kJ/mol) present at the beginning of the pore, which corresponds to the Arg294 in the B subunit (here, the potential is positive and the radius of the pore smaller). The second profile type groups together the homopentamer 5-HT_{3B}R and the "ABBBB", "AABBB" and "BBABA" heteropentamers. These receptors have in common a positive pore surface potential (see Electrostatic potential surface section), that is consistent with a non favourable PB energy profile showed in Fig. 8c. The peaks are in the same regions of those of the homopentamer 5-HT_{3A}R and the "AAAAB" heteropentamer, but have a major intensity, which increases with the number of B subunits. This type of profile, similar to that of the chloride ion through the 5-HT_{3A}R, suggests the presence of a high energy barrier that contrasts the cations passage through the pore, and confirms the results obtained from the analysis of the MEPs (see Electrostatic potential surface section). Finally, the third profile type groups the last two heteropentamers, "ABABA" and "AAABB", which are characterized by a negative pore surface MEP (see Electrostatic potential surface section) and for which it was expected a PB energy profile not too different from that of the homopentamer 5-HT_{3A}R or that of the "AAAAB" heteropentamer. Differently from what expected, their PB energy profiles show a series of peaks, in particular at the channel entrance (Pore Axis $z > 90$ Å), that are not present in the PB energy profiles of the other receptors (Fig. 8d). Furthermore, what was mainly unexpected is the totally unfavourable interaction energy profile, which is difficult to explain given the negative pore MEP of the "ABABA" and "AAABB" heteropentamers. The calcium ion should encounter a favourable attraction while entering the channel; conversely, it seems to be repelled by the channel in these two receptors, as testified by the several energetic barriers it encounters. Thus, further analyses of these receptors seem to be necessary to clarify the unexpected behaviour of the "ABABA" and "AAABB" heteropentamers. Probably, in this case, the limitations of the PB method become important and prevent a correct interpretation and analysis of the receptors features and/or the presence of the EC domain receptor structure, not considered in this work, exerts important modification both on the structure and the electrostatic properties of the TM domain.

In summary, it has been shown that the hydrophobic belt at the centre of the 5-HT_3R pore acts as a hydrophobic gate, increasing the energy barrier encountered by a putative calcium ion moving through the channel. Moreover, the homopentamer 5-HT_{3A}R and the heteropentamer 5-HT_{3AB}R with stoichiometry "AAAAB", have very similar PB energy profiles, which are consistent with the MEP features and with the experimental results on 5-HT_3R [65, 66, 69] and on nAChR [14, 86]. The homopentamer 5-HT_{3B}R and the heteropentamer 5-HT_{3AB}Rs with the stoichiometries "ABBBB", "AABBB" and "BBABA" share a similar PB energy profile, which is not favourable to the cations passage, suggesting that these receptors are non-functional and confirming the results obtained from the MEP analysis. Finally, for the heteropentamer 5-HT_{3AB}Rs with the stoichiometries "ABABA" and "AAABB" further analysis are required to understand their unexpected behaviour.

Conclusions

The results of the structural and functional characterisation studies carried out by means of computational studies on the TM and IC domains of the 5-HT_3 receptor family have been successful in providing new insights into the stoichiometric composition of functional receptors. A complete view of the receptor, including the EC domain, might however be useful to clarify few unexpected findings (i.e. the "ABABA" and "AAABB" heteropentamers pore profile) and peculiar cases (i.e. the potential functionality of the "BBABA" heteropentamers, for which previous analysis of the electrostatics properties of the isolated EC domain led to contrasting conclusions).

The electrostatic potential map analysis computed on the surfaces of the 3D structure of the five modelled TM-IC domain subunits (5-HT_3 A to E) corroborates two major structural differences, previously highlighted on the basis of the analyses of the amino acids sequence: i) subunit B

might be ion-unselective since it lacks the charged residue commonly found at the TM2 position -1, which is critical for ion selectivity; ii) the experimentally demonstrated low channel conductance of subunit A might be due to the peculiar presence of three Arg in the MA-helix (R-4′, R0′ and R4′), which are not found in any of the other subunits.

Furthermore, this analysis provides a static picture of the environment that an ion encounters when passing through the pore at the TM and IC domain levels and suggests that the negative pore potential surface, required for the ions to enter the channel and cross it, is granted by the maximum presence of two B subunits (although some exception might be envisaged) in the 5-HT_3AB receptors. This hypothesis is further confirmed by the analysis of the energetic profile of a selected ion along the pore channel of 5-HT_3 homopentamer A and B and of 5-HT_3AB heteropentamers, estimated by using the Poisson-Boltzmann (PB) equation.

References

1. Hannon J, Hoyer D (2008) Molecular biology of 5-HT receptors. Behav Brain Res 195:198–213
2. Parthiban M, Rajasekaran MB, Ramakumar S, Shanmughavel PJ (2009) Molecular modeling of human pentameric alpha(7) neuronal nicotinic acetylcholine receptor and its interaction with its agonist and competitive antagonist. J Biomol Struc Dyn 26:535–547
3. Peters JA, Hales TG, Lambert JJ (2005) Molecular determinants of a single channel conductance and ion selectivity in the Cys-loop family: insights from the 5-HT_3 receptor. Trends Pharmacol Sci 26:587–594
4. Unwin N (2005) Refined structure of the nicotinic acetylcholine receptor at 4 Å resolution. J Mol Biol 346:967–989
5. Hilf RJC, Dutzler R (2008) X-ray structure of a prokaryotic pentameric ligand-gated ion channel. Nature 452:375–380
6. Bocquet N, Nury H, Baaden M, Le Poupon C, Changeux JP, Delarue M, Corringer PJ (2009) X-ray structure of a pentameric ligand-gated ion channel in an apparently open conformation. Nature 457:111–114
7. Hibbs RE, Gouaux E (2011) Principles of activation and permeation in an ion-selective Cys-loop receptor. Nature 474:54–60
8. Barnes NM, Hales TG, Lummis SCR, Peters JA (2009) The 5-HT_3 receptor: the relationship between structure and function. Neuropharm 56:273–284; and references therein
9. Boess FG, Beroukhim R, Martin IL (1995) Ultrastructure of the 5-hydroxytryptamine$_3$ receptor. J Neurochem 64:1401–1405
10. Karlin A (2002) Emerging structure of the nicotinic acetylcholine receptors. Nat Rev Neurosci 3:102–114
11. Reeves DC, Lummis SCR (2002) The molecular basis of the structure and function of the 5-HT_3 receptor: a model ligand-gated ion channel. Mol Memb 9:11–26
12. Lester HA, Dibas MI, Dahan DS, Leite JF, Dougherty DA (2004) Cys-loop receptors: new twists and turns. Trends Neurosci 27:329–336
13. Sine SM, Engel AG (2006) Recent advances in Cys-loop receptor structure and function. Nature 440:448–455
14. Miyazawa A, Fujiyoshi Y, Unwin N (2003) Structure and gating mechanism of the acetylcholine receptor pore. Nature 423:949–955
15. Barry PH, Lynch JW (2005) Ligand-garted channels. IEEE Trans Nanobiosci 4:71–80
16. Unwin N, Fujiyoshi Y (2012) Gating movement of acetylcholine receptor caught by plunge-freezing. J Mol Biol 422:617–634
17. Bouzat C (2012) New insights into the structural bases of activation of Cys-loop receptors. J Physiol Paris 106:23-33; and refs. therein
18. Liu X, Xu Y, Li H, Wang X, Jiang H, Barrantes FJ (2008) Mechanics of channel gating of the nicotinic acetylcholine receptor. PLoS Comp Biol 4:100–110
19. Taly A (2007) Opened by a twist: a gating mechanism for the nicotinic acetylcholine receptor. Eur Biophys J 36:911–918
20. Nury H, Poitevin F, Van Renterghem C, Changeux JP, Corringer PJ, Delarue M, Baaden M (2010) One-microsecond molecular dynamics simulation of channel gating in a nicotinic receptor homologue. Proc Natl Acad Sci USA 107:6275–6280
21. Filatov GN, White MM (1995) The role of conserved leucines in the M2 domain of the acetylcholine receptor in channel gating. Mol Pharmacol 48:379–384
22. Corringer PJ, Le Novere N, Changeaux JP (2000) Nicotinic receptors at the amino acid level. Ann Rev Pharmacol Toxicol 40:431–458
23. Nielser B, Walstab J, Combrink S, Moller D, Kapeller J, Rietdorf J, Bonish H, Gothert M, Rappold G, Bruss M (2007) Characterisation of the novel human serotonin receptor subunits 5-HT_{3C}, 5-HT_{3D} and 5-HT_{3E}. Mol Pharmacol 72:8–17
24. Holbrook JD, Gill CH, Zebda N, Spencer JP, Leyland R, Rance KH, Trin H, Balmer G, Kelly FM, Yusaf SP, Courtenay N, Luck J, Rhodes A, Modha S, Moore SE, Sanger GJ, Gunthorpe MJ (2009) Characterisation of 5-HT_{3C}, 5-HT_{3D} and 5-HT_{3E} receptor subunits: evolution, distribution and function. J Neurochem 108:384–396
25. Boyd GW, Low P, Dunlop JI, Robertson LA, Vardy A, Lambert JL, Peters JA, Connolly CN (2002) Assembly and cell surface expression of homomeric and heteromeric 5-HT_3 receptors: the role of oligomerization and chaperone proteins. Mol Cell Neurosci 21:38–50
26. Barrera NP, Herbert P, Henderson RM, Martin IL, Edwardson JM (2005) Atomic force microscopy reveals the stoichiometry and subunit arrangement of 5-HT_3 receptors. PNAS 102:12595–12600
27. Lochner M, Lummis SCR (2010) Agonists and antagonists bind to an A–A interface in the heteromeric 5-HT_3AB receptor. Biophys J 98(8):1494–1502
28. Thompson AJ, Price KL, Lummis SCR (2011) Cysteine modification reveals which subunits form the ligand binding site in human heteromeric 5-HT_3AB receptors. J Physiol 589:4243–4257
29. Menziani MC, De Rienzo F, Cappelli A, Anzini M, De Benedetti PG (2001) A computational model of the 5-HT_3 receptor extracellular domain: search for ligand binding sites. Theor Chem Acc 106:98–104
30. Joshi PR, Suryanarayanan A, Hazai E, Schulte MK, Maksay G, Bikàdi Z (2006) Interactions of granisetron with an agonist-free 5HT_{3A} receptor model. Biochem 45:1099–1105
31. Moura Barbosa AJ, De Rienzo F, Ramos MJ, Menziani MC (2010) Computational analysis of ligand recognition sites of homo- and heteropentameric 5-HT_3 receptors. Eur J Med Chem 45(11):4746–4760
32. Cappelli A, Manini M, Paolino M, Gallelli A, Anzini M, Mennuni L, Del Cadia M, De Rienzo F, Menziani MC, Vomero S (2011) Bivalent ligands for the serotonin 5-HT_3 receptor. ACS Med Chem Lett 2(8):571–576
33. De Rienzo F, Moura Barbosa AJ, Perez MAS, Fernandes PA, Ramos MJ, Menziani MC (2012) The extracellular subunit interface of the 5-HT_3 receptors: a computational alanine scanning mutagenesis study. J Biomol Struct Dyn 30(3):280–298

34. De Rienzo F, Del Cadia M, Menziani MC (2012) A first step towards the understanding of the 5-HT_3 Receptor subunit heterogeneity from a computational point of view. Phys Chem Chem Phys 14(36):12625–12636
35. Dey R, Chen LJ (2011) In search of allosteric modulators of a7-nAChR by solvent density guided virtual screening. J Biomol Struct Dyn 28:695–715
36. Parthiban M, Shanmughavel P, Sowdhamini R (2010) In silico point mutation and evolutionary trace analysis applied to nicotinic acetylcholine receptors in deciphering ligand-binding surfaces. J Mol Mod 16:1651–1670
37. Subramanian S, Mohmmed SA, Gupta D (2009) Molecular modeling studies of the interaction between plasmodium falciparum HslU and HslV subunits. J Biomol Struct Dyn 26:473–479
38. Ortells MO, Barrantes GE (2008) A model for the assembly of nicotinic receptors based on subunit–subunit Interactions. Proteins 70:473–488
39. Price KL, Lummis SCR (2004) The role of tyrosine residues in the extracellular domain of the 5-hydroxytryptamine$_3$ receptor. J Biol Chem 279:23294–23301
40. Price KL, Bower KS, Thompson AJ, Lester HA, Dougherty DA, Lummis SCR (2009) A hydrogen bond in loop A is critical for the binding and function of the 5-HT_3 receptor. Biochem 47:6370–6377
41. Sullivan NL, Thompson AJ, Price KL, Lummis SCR (2006) Defining the roles of Asn-128, Glu-129 and Phe-130 in loop A of the 5-HT_3 receptor. Mol Membr Biol 23(5):442–451
42. Thompson AJ, Lochner M, Lummis SCR (2008) Loop B is a major structural component on the 5HT_3 receptor. Biophys J 95:5728–5736
43. The UniProt Consortium (2008) The universal protein resource (Uniprot). Nucleic Acids Res 36:D190–D195
44. Zhu F, Hummer G (2012) Theory and simulation of ion conduction in the pentameric GLIC channel. J Chem Theory Comput 8:3759–3768
45. Thompson JD, Higgins DG, Gibson TJ, Clustal W (1994) Improving the sensitivity of progressive multiple sequence alignment through sequence weighting, position-specific gap penalties, and weight matrix choice. Nucleic Acids Res 22:4673–4680
46. Sali A, Blundell TL (1993) Comparative protein modelling by satisfaction of spatial restraints. J Mol Biol 234:779–815
47. Krogh A, Larsson B, von Heijne G, Sonnhammer EL (2001) Predicting transmembrane protein topology with a hidden Markov model: application to complete genomes. J Mol Biol 305(3):567–580
48. Buchan DW, Ward SM, Lobley AE, Nugent TC, Bryson K, Jones DT (2010) Protein annotation and modelling servers at University College London. Nucl Acids Res 38:W563–W568
49. Jones DT (1999) Protein secondary structure prediction based on position-specific scoring matrices. J Mol Biol 292:195–202
50. Laskowski RA, MacArthur MW, Moss DS, Thornton JM (1993) PROCHECK: a program to check the stereochemical quality of protein structure. J Appl Cryst 26:283–291
51. Colovos C, Yates TO (1993) Verification of protein structures: patterns of nonbonded atomic interactions. Protein Sci 2(9):1511–1519
52. Hooft RWW, Vriend G, Sander C, Abola EE (1996) Errors in protein structures. Nature 381:272–273
53. Vriend G (1990) WHAT IF: a molecular modeling and drug design program. J Mol Graph 8:52–56
54. Baker NA, Sept D, Joseph S, Holst MJ, McCammon JA (2001) Electrostatics of nanosystems: application to microtubules and the ribosome. Proc Natl Acad Sci 98:10037–10041
55. DeLano WL (2008) PyMOL molecular graphics system. DeLano Scientific LLC, Palo Alto
56. Lerner MG, Carlson HA (2006) APBS plugin for PyMOL. University of Michigan, Ann Arbor
57. Dolinsky TJ, Nielsen JE, McCammon JA, Baker NA (2004) PDB2PQR: an automated pipeline for the setup, execution, and analysis of Poisson-Boltzmann electrostatics calculations. Nucleic Acids Res 32:W665–W667
58. Dolinsky TJ, Czodrowski P, Li H, Nielsen JE, Jensen JH, Klebe G, Baker NA (2007) PDB2PQR: expanding and upgrading automated preparation of biomolecular structures for molecular simulations. Nucleic Acids Res 35:W522–W525
59. Tai K, Fowler P, Mokrab Y, Stansfeld P, Sansom MSP (2008) Molecular modeling and simulation studies of ion channel structures, dynamics and mechanisms. Meth Cell Biol 90(12):233–265
60. Smart OS, Neduvelil JG, Wang X, Wallace BA, Sansom MS (1996) HOLE: a program for the analysis of the pore dimensions of ion channel structural models. J Mol Graph 14(6):354-60, 376
61. Rashin A, Hoing B (1985) Reevaluation of the Born model of ion hydration. J Phys Chem 89:5588
62. Beckstein O, Tai K, Sansom MSP (2004) Not ions alone: barriers to ion permeation in nanopores and channels. J Am Chem Soc 126:14694–14695
63. Tai K, Haider S, Grottesi A, Sansom MSP (2009) Ion channel gates: comparative analysis of energy barriers. Eur Biophys J 38:347–354
64. Humphrey W, Dalke A, Schulten K (1996) VMD: visual molecular dynamics. J Mol Graph 14:33–38
65. Gunthorpe MJ, Lummis SCR (2001) Conversion of the ion selectivity of the 5-HT_{3A} receptor from cationic to anionic reveals a conserved feature of the ligand gated ion channel superfamily. J Biol Chem 276:10977–10983
66. Thompson AJ, Lummis SCR (2003) A single ring of charged amino acids at one end of the pore can control ion selectivity in the 5-HT_3 receptor. Br J Pharmacol 140:359–365
67. Yakel JL, Lagrutta A, Adelman JP, North RA (1993) Single amino acid substitution affects desensitization of the 5-hydroxytryptamine type 3 receptor expressed in *Xenopus oocytes*. Proc Natl Acad Sci 90:5030–5033
68. Gunthorpe MJ, Peters JA, Gill CH, Lambert JJ, Lummis SC (2000) The 4′lysine in the putative channel lining domain affects desensitization but not the single-channel conductance of recombinant homomeric 5-HT3A receptors. J Physiol 522:187–198
69. Paniker S, Cruz H, Arrabit C, Slesinger A (2002) Evidence for a centrally located gate in the pore of a serotonin-gated ion channel. J Neurosci 22:1629–1639
70. Dang H, England PM, Farivar SS, Dougherty DA, Lester HA (2000) Probing the role of a conserved M1 proline residue in 5-hydroxytriptamine$_3$ receptor gating. Mol Pharmacol 57: 1114–1122
71. Sessoms-Sikes JS, Hamilton ME, Liu LX, Lovinger DM, Machu TK (2003) A mutation in transmembrane domain II of the 5-hydroxytryptamine(3A) receptor stabilizes channel opening and alters alcohol modulatory actions. J Pharmacol Exp Ther 306:595–604
72. Livesey MR, Cooper MA, Deep TZ, Carland JE, Kozuska J, Hales TG, Lambert JJ, Peters JA (2008) Structural determinants of Ca^{2+} permeability and conduction in the human 5-HT_3A receptor. J Biol Chem 282:6172–6182
73. Kelley SP, Dunlop JI, Kirkness EF, Lambert JJ, Peters JA (2003) A cytoplasmic region determines single-channel conductance in 5-HT_3 receptors. Nature 424:321–324
74. Hales TG, Dunlop JI, Deeb TZ, Carland JE, Kelley SP, Lambert JJ, Peters JA (2006) Common determinants of single channel conductance within the large cytoplasmic loop of 5-hydroxytriptamine type 3 and $\alpha4\beta2$ nicotinic acetylcholine receptors. J Biol Chem 281:8062–8071
75. Peters JA, Cooper MA, Carland JE, Livesey MR, Hales TG, Lambert JJ (2010) Novel structural determinants of single channel

conductance and ion selectivity in 5-hydroxytryptamine type 3 and nicotinic acetylcholine receptors. J Physiol 588(4):587–595
76. Kienker P, Tomaselli G, Jurman M, Yellen G (1994) Conductance mutations of the nicotinic acetylcholine receptor do not act by a simple electrostatic mechanism. Biophys J 66:325–334
77. Corringer PJ, Bertrand S, Galzi JL, Devillers-Thiery A, Changeux JP, Bertrand D (1999) Mutational analysis of the charge selectivity filter of the alpha7 nicotinic acetylcholine receptor. Neuron 22:831–843
78. Cymes GD, Grosman C (2011) Tunable pK_a values and the basis of opposite charge selectivities in nicotinic-type receptors. Nature 474:526–530
79. Tapia L, Kuryatov A, Lindstrom J (2007) Ca^{2+} permeability of the $(\alpha 4)_2(\beta 2)_3$ human acetylcholine receptors. Mol Pharmacol 71:769–776
80. Davies PA, Pistis M, Hanna MC, Peters JA, Lambert JJ, Hales TG, Kirkness EF (1999) The 5-HT_{3B} subunit is a major determinant of serotonin receptor function. Nature 397:359–363
81. Walstab J, Rappold G, Niesler B (2010) 5-HT_3 receptors: role in disease and target of drugs. Pharm Therap 128:146–169
82. Parsegian A (1969) Energy of an ion crossing a low dielectric membrane: solutions to four relevant electrostatic problems. Nature 221:844–846
83. Partenskii MB, Jordan PC (1992) Theoretical perspectives on ion-channel electrostatics: continuum and microscopic approaches. Q Rev Biophys 25:477–510
84. Kuyucak S, Hoyles M, Chung S (1998) Analytical solutions of Poisson's equation for realistic geometrical shapes of membrane ion channels. Biophys J 74(1):22–36
85. Mokrab Y, Bavro VN, Mizuguchi K, Todorov NP, Martin IL, Dunn SMJ, Chan SL, Chau PL (2007) Exploring ligand recognition and ion flow in comparative models of the human GABA type A receptor. J Mol Graph Model 26:760–774
86. Amiri S, Tai K, Beckstein O, Biggin PC, Sansom MSP (2005) The α7 nicotinic acetylcholine receptor: molecular modelling, electrostatics, and energetic. Mol Membr Biol 22(3):151–162
87. Beckstein O, Sansom MSP (2006) A hydrophobic gate in an ion channel: the closed state of the nicotinic acetylcholine receptor. Phys Biol 3:147–159